ChemTexts (2015) 1:5
DOI 10.1007/s40828-014-0005-6

LECTURE TEXT

Dating: an analytical task

Antonio Doménech-Carbó

Received: 6 October 2014 / Accepted: 26 December 2014 / Published online: 31 January 2015

Abstract Dating of archeological and geological materials is an important task in the fields of history, anthropology, archeology, geology, paleontology, etc. which can be achieved from a variety of sources of information from historical and astronomical to biological. Within the wide variety of such scientific sources of information, physical and chemical methods of dating play an essential role and, to a great extent, they share the same general methodologies which are applied in analytical chemistry. The basis of the main physical and chemical methods of dating is discussed with particular attention to calibration and error estimation.

Keywords Dating · Analytical chemistry · Radiocarbon · Chemical methods

Preface

We experience time based on our perception of events and our memory of the events in the past and associate time duration to repetitive events but our ability to comprehend duration remains ultimately subjective, biased by the conditions of our individual experience.

The development of science relies, to some extent, on the 'invention' or 'construction' of an 'external', 'objective' concept of time. As discussed by Burchfield [1], geological time was a construct, an 'artifact', created from the vague notion of 'deep time' associated with a view of the Earth as an evolutionary system, particularly prompted by Hutton[1] and Lyell.[2] The next steps of the construction of the geological time involved the development of a heuristic geological timescale representative of the Earth's history, the creation of quantitative methods to calculate the units of that scale, and the acceptance of a quantitatively determinable limit of the age of the Earth [1].

Astronomical time is based on the repetition of astronomical phenomena. Although these phenomena are not exactly repetitive in terms of contemporary atomic time scales, they are important because of their use in calendars as well as for observers on the Earth needing to determine the orientation of our planet in an inertial reference frame, namely, navigators, astronomers and geodesists [2].

In the field of physics, the concept of time was dominated by the Newtonian view of an absolute (universal, homogeneous) time inextricably following from the concept of absolute space. In the Principia [3], Newton wrote:

> "Absolute, true, and mathematical time, of itself, and from its own nature flows equably without regard to anything external, and by another name is called duration: relative, apparent, and common time, is some sensible and external (whether accurate or unequable) measure of duration by the means of motion, which is commonly used instead of true time; such as an hour, a day, a month, a year."

The universal Newtonian time, flowing uniformly, whereas the material bodies experience different processes

Electronic supplementary material The online version of this article (doi:10.1007/s40828-014-0005-6) contains supplementary material, which is available to authorized users.

A. Doménech-Carbó (✉)
Departament de Química Analítica, Universitat de València, Dr. Moliner, 50, 46100 Burjassot, València, Spain
e-mail: Antonio.Domenech@uv.es

[1] James Hutton (3 June 1726–26 March 1797). Scottish geologist.

[2] Charles Lyell (14 November 1797–22 February 1875). British geologist and close friend of Charles Darwin.

in an empty, absolute space, is one of the essential elements of the paradigm of classical mechanics. The Newtonian time still remains, probably, as an implicit conceptual background for the contemporary view of dating but the concept of time has been significantly revised in the relativistic theories and in quantum mechanics [4, 5].

For our purposes, the relevant point to underline is that dating can be considered as a procedure for fixing a given phenomenon, the fabrication of an artifact, the minting of a coin, the death of an organism, on a standardized time scale, thus providing valuable information for historical, archeological, geological purposes, etc. This requires to have a clock, i.e., a suitable procedure for measuring time and to know the zero-setting. The zero setting, for instance the death of a living organism in radiocarbon dating, is the event defining the initiation of the time-counting process. Obviously, this 'time zero' has to be placed on a calendrical time scale via calibration with events of known age in that calendrical time scale. All dating procedures (astronomical, biological, stylistic, etc.) can be viewed, in a broad sense, as analytical tasks, requiring the reception and interpretation of empirical data in the context of a defined conceptual frame (historical, linguistic, etc.) aimed to obtain conclusions on the origin, duration, age, etc. of the observed phenomena. Among them, dating methods involving the use of the basic principles of physics (radiocarbon dating, isotope abundance ratios, etc.), or chemistry (e.g., aminoacid racemization), play an essential role for dating purposes. Such methods of dating have in common with analytical chemistry methods the general structure of the analytical process (sampling, determination, data analysis, etc.) as well as much of the operational aspects involved in such process [6]. The current text, although concerned with a generalized view of dating, will be focused on the physical and chemical methods of dating. Dating is a topic which can enrich the curricula of analytical chemistry.

Dating: an overview

Dating methods

The dating methods are usually divided into absolute and relative. For Wagner [7], absolute methods are those allowing to fix the age of an object or event to a certain point on a defined time scale (for example a piece of wood dated by ^{14}C to 1000 BC) whereas relative methods tell something about the age of an object or event in relation to another (for example the stratigraphy of a geological site allows distinguishing between younger, older or the same age). The above definition is slightly different from that of Aitken [8] for which absolute dating methods are those providing the age of an object or the time passed since a certain event or event relative to a standardized calendar independently of any other dating technique. Relative (or indirect or derivative) dating provides a time interval and organizes events or materials in time series without fixing a zero time of the calendar.

Constructing a sound chronology is an interdisciplinary task. For instance, historical dating of Egyptian and Mesopotamian cultures based on astronomical records involves the knowledge of such diverse fields as astronomy, Semitic languages, Egyptian hieroglyphs, ceramics, and field archeology. In favorable cases, different methods of dating can be combined (for instance, radiocarbon dating of ancient papyrus and astronomical data contained in the same) to obtain chronological information.

Of course, the sources of information for dating can be diverse. For instance, in the field of archeology, dating can be performed based on epigraphy (analysis of inscriptions and graphemes), paleography (analysis of written documents), numismatics and stylistic analysis. In the field of geology, fossil markers, in particular, pollen (palynology) and foraminifera and growth marks (dendrochronology, acanthochronology, etc.) are routinely used. In both the fields of geology and archeology, stratigraphic analysis provides the time sequence of formation of the different layers. Apart from morphological and compositional properties of the strata, several stratigraphic markers can be used, for instance, paleomagnetism[3] and tephrochronology.[4] Here, dating based on the measurement of some physical property and/or the chemical composition of the sample under study will be preferentially discussed.

It is pertinent to note, however, that the physical and chemical techniques of analysis can be applied not only to the direct study of an artifact but also to other materials which accompany the object such as residuals, surrounding soil, etc. For instance, dating archeological metal can be performed when organic residuals accompany the studied artifact. In general, the application of dating techniques involves a measurable time-dependent quantity and an event which determines the start of the time-counting. It should be kept in mind that dating involves the introduction of a chronology into a given calendar, but not all the calendars are equivalent.

There are several possible criteria for classifying the methods of dating. In Fig. 1, the main physical and chemical methods are grouped on the basis of the physical mechanisms defining the 'clock' and/or the measurement

[3] Paleomagnetism is the ensemble of phenomena associated to the Earth's magnetic field in rocks and archeological materials.

[4] Tephrochronology is a geochronological technique that uses discrete layers of volcanic ash from a single eruption (tephra) in order to establish a chronology.

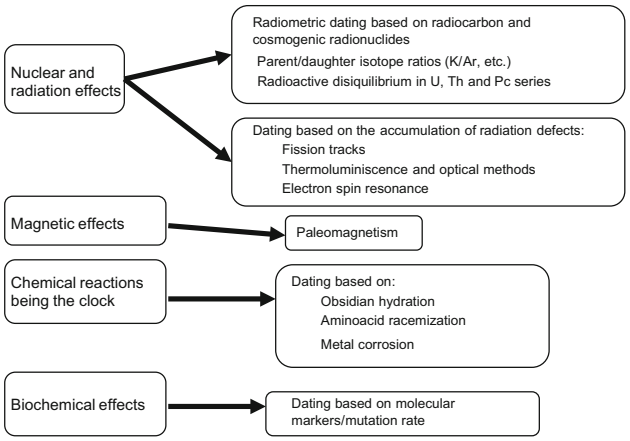

Fig. 1 Main physical and chemical methods used in geological and archeological dating grouped on the basis of the physical mechanisms defining the 'clock' and/or the measurement technique

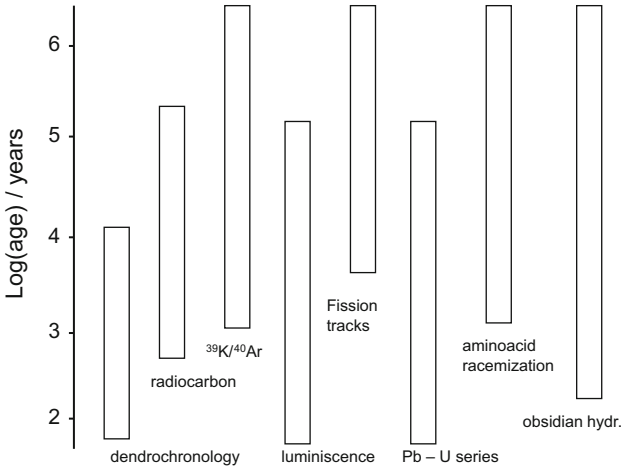

Fig. 2 Comparison of the typical age ranges available for several dating techniques

techniques. Obviously, the classification given in Fig. 1 is somehow arbitrary, but can be used as an overview.

Here, the main physical and chemical methods will be presented following an operational criterion: their implementation as analytical methods directly addressed to date geological and/or archeological samples and related to analytical chemistry methodologies. By reasons of space and specificity, astronomical, epigraphic, etc., methods of dating as well as paleomagnetic phenomena will not be treated. By the same reasons, biological molecular clocks will be only briefly commented. Overall, physical and chemical methods of dating can be seen as analytical methods and hence submitted to the usual rules regarding the so-called analytical properties: accuracy and precision, sensitivity, selectivity, repeatability, reproducibility, robustness, security, traceability, etc. of application in analytical chemistry. Of particular importance in the analytical process are the steps of sampling (representativity and integrity of the sample) as well as the operations of calibration and analysis of errors. These two important aspects will be treated as an Appendix ("Appendix 1").

It is convenient to mention that physical methods based, for instance, on the radioactive clock would be, in principle, more reliable than chemical methods because radioactive decays are independent of temperature, pressure, and concentration. In practice, however, nuclear clocks can also be affected by environmental factors, because parent and daughter isotopes may migrate into or out of the sample.

Geological and archeological clocks

The different methods of dating cover different phenomena and are applicable for different intervals of time, as illustrated in Fig. 2. Accordingly, the method for determining the age of a given archeological or geological sample has to be selected depending on the range of ages accessible to each method. Such methods are based on the study of a given time-dependent feature, the geological or archeological clock, able to provide an age for the sample under study. In most cases, two or more dating methods are available for dating a given sample so that a consistent set of dating can be obtained. It is pertinent to note that dating requires an accurate calibration and that the uncertainty associated with the age estimated for a given object can vary significantly depending on its age, method and a variety of factors.

Dating based on cosmogenic isotopes

General considerations

An important family of dating methods is based on monitoring the concentration and radioactivity of cosmogenic[5] isotopes: those formed in the Earth as a result of nuclear reactions between stable isotopes and cosmic radiation (or possibly other sources). When radioactive isotopes are generated, as is the case of carbon-14, the radioactive decay of such isotopes provides a direct basis for dating. When stable isotopes are generated, their abundance relative to other isotopes can be used for chronological purposes.

[5] The word "cosmogenic" derives from the word "cosmos" (Latin, Greek), here meaning the universe outside the Earth, and "genesis" (Latin, Greek) meaning creation. Thus, cosmogenic nuclides means here "nuclides created by cosmic rays", in opposition to "primordial nuclides", which have existed on Earth since before the Earth was formed.

Fig. 3 Photographic image of Victor F. Hess. At 7 August 1912, he identified the existence of a pervasive radiation, further labeled as cosmic radiation, in 5300 meters altitude above the Schwieloch Lake in the southeast of Brandenburg. Photograph from Bettmann/Corbis, with permission

Cosmic rays, which were discovered in 1912 by the Austro-American physicist Victor Franz Hess[6] (see Fig. 3), consist of particles, mainly protons, and gamma rays which arrive to the Earth from external sources, the Sun in particular. Primary cosmic rays, which are those arriving to the external atmosphere, are formed by particles whose energy ranges between 1 GeV (10^9 eV) and 10^{13} eV. Such primary cosmic radiation has an isotropic distribution and an essentially constant intensity at heights above 50–60 km. Secondary cosmic rays are formed as a result of the impact of the primary cosmic radiation with the atmospheric components giving rise to a variety of particles. The 'hard', highly penetrating component of the secondary cosmic rays is formed mainly by muons resulting form the disintegration of π mesons (pions). The 'soft' components are mainly electrons, positrons and photons.

Table 1 summarizes the properties of the primary cosmic radiation [9]. The flux density represents the number of particles per unit of time, unit of surface and unit of solid angle reaching the atmosphere. The rate of production of cosmogenic isotopes depends on the concentration of the target elements, the elevation, latitude and other 'local' factors.

Radiocarbon dating

Foundations of radiocarbon dating

Radiocarbon dating, invented by Libby[7] (Fig. 4) in the late 1940s [10–12], is based on the fact that the radioactive isotope of carbon of mass number 14, in the following denoted as radiocarbon or ^{14}C, is constantly formed in the Earth's atmosphere by the interaction of secondary cosmic rays with atmospheric nitrogen yielding mostly radioactive carbon dioxide. As previously indicated, our planet is under constant bombardment by cosmic radiation, mainly composed of protons, coming from the Sun, accompanied by energetic particles originating largely from our own galaxy and even from sources outside the Milky Way.

Such high-energy particles are responsible for generating secondary cosmic radiation, also rich in neutrons, which interacts with target elements in the atmosphere and the Earth's surface to produce cosmogenic nuclides. ^{14}C is generated according to the reaction:

$$^{14}_{7}N + {}^{1}_{0}n \rightarrow {}^{14}_{6}C + {}^{1}_{1}H \quad (1)$$

The ^{14}C atoms are oxidized in the atmosphere to $^{14}CO_2$, and the ^{14}C is incorporated into plants by photosynthesis and subsequently is passed to animals. Atmospheric carbon dioxide also enters into the oceans as dissolved CO_2 and HCO_3^-/CO_3^{2-}.

The radiocarbon experiences a radioactive decay according to:

$$^{14}_{6}C \rightarrow {}^{14}_{7}N + e + \bar{\upsilon}_e \quad (2)$$

by emitting a beta particle (electron) and an electron antineutrino.

The isotopic composition of carbon in the atmosphere is constant because of the constant formation and decaying of ^{14}C. This situation is parallel to that described in chemical kinetics, as schematized in Fig. 5. Thus, let us consider that the formation of a daughter radioactive isotope B from a parent stable atmospheric (or another reservoir such as soil, biosphere, etc.) isotope A started at a time zero when the concentration of the parent atmospheric isotope was c_0. Assuming that the formation of B from A follows a first-order kinetics and that the radioactive isotope B decays following the usual rate law, the net concentration of A and

[6] Victor Franz Hess (June 1883–December 1964), Austrian physicist naturalized United States citizen in 1944, shared the Nobel Prize in 1936 by his discovery of cosmic rays.

[7] Willard Frank Libby (Grand Valley, 1908–Los Angeles, 1980) was awarded with the Nobel prize in 1960 for the development of the radiocarbon method of dating. The collected papers of Libby are available: Libby WF (1982) Collected Papers. Geo Science Analytical, Santa Monica, Vol 1–7.

Table 1 Composition and flux density of the different fractions of nuclei forming the primary cosmic radiation [9]

Group of particles	Z	Flux density (m^{-2} sr^{-1} s^{-1})	Flux (%)
Protons	1	1,300	92.9
He	2	88	6.3
Light particles	3–5	1.9	0.13
Medium particles	6–9	5.6	0.4
Heavy particles	≥10	2.5	0.18
Super-heavy particles	≥20	0.7	0.05

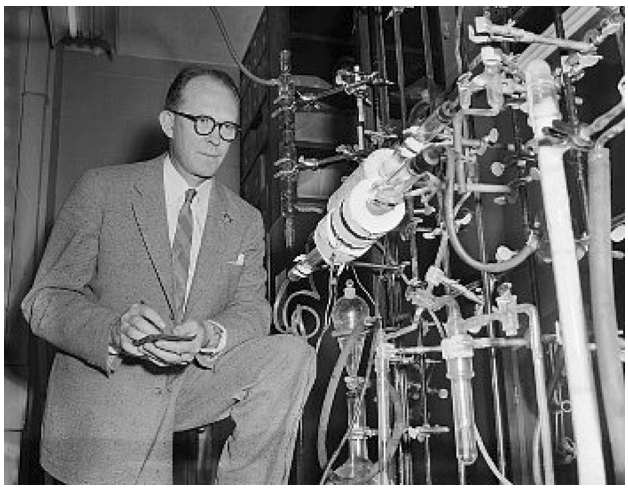

Fig. 4 Willard Libby in his laboratory. 15th September 1954. Photograph of Bettmann/Corbis, with permission

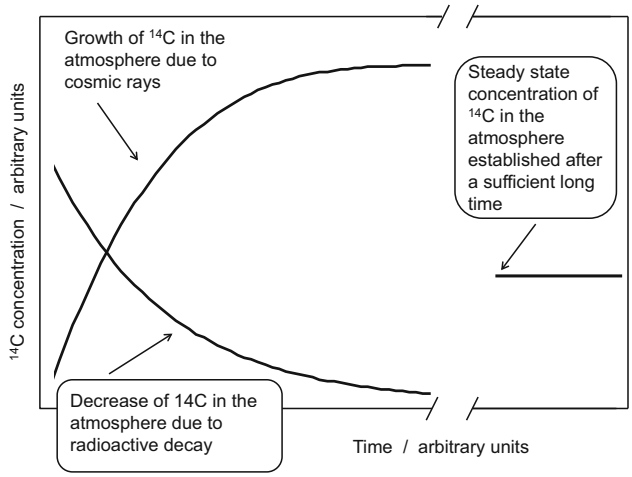

Fig. 5 Representation of the formation and depletion of carbon-14 in the atmosphere

B at a time t in the atmosphere, c_A, c_B, respectively, is given by the expressions:

$$\frac{dc_A}{dt} = -kc_A; \quad \frac{dc_B}{dt} = kc_A - \lambda c_B; \quad \frac{dc_C}{dt} = \lambda c_B \qquad (3)$$

where k denotes the rate constant for the reaction of formation of B and λ the radioactive decay constant of B. Integration of these equation yields:

$$c_A = c_0 \exp(-kt); \quad c_B = \frac{kc_o}{(\lambda - k)}\{e^{-kt} - e^{-\lambda t}\} \qquad (4)$$

If a large excess of A exists in the atmosphere, the ratio between the concentrations of B and A tends, at sufficiently long times to a constant value given by:

$$c_B/c_A \approx k/\lambda \qquad (5)$$

In general, there are other nuclear reactions giving rise to the formation of the isotope B and the depletion of such isotope in the atmosphere (or the considered reservoir) can be produced not only by radioactive decay but also from other nuclear processes. Apart from the above, the concentration of B in the atmosphere can vary due to exchange processes with other reservoirs. In the case of radiocarbon dating, it is assumed that the rate of formation of ^{14}C in the atmosphere as a result of the action of cosmic rays equals the rate of depletion as a result of radioactive decay and exchange with living organisms, oceans, etc. A similar scheme could be applied to living organisms where the concentration of ^{14}C can be considered as a constant.

When the animal or plant dies, the process of accumulating (and exchanging) carbon is stopped and no new ^{14}C can be incorporated, and then the ^{14}C content can only exponentially decrease with time as a result of radioactive decay. Accordingly, the carbon-14 activity of a sample of age t years, A, satisfies the relationship (for derivation of this equation, see [13]):

$$A = A_0 \exp(-\lambda t) \qquad (6)$$

In this equation, A_0 represents the activity at time zero and λ is the radioactive constant, characteristic of the radioactive decay process, which equals the inverse of the mean-life (or lifetime), τ, of the isotope [8,267 years for the process described by Eq. (2)]. The radioactive constant is related to the half-life, $t_{1/2}$, defined as the time required for diminishing the activity of a radiocarbon sample to its half, according to:

$$t_{1/2} = \frac{\ln 2}{\lambda} = \frac{0.693}{\lambda} \qquad (7)$$

The currently accepted value of $t_{1/2}$ is 5,730 ± 40 years. Equation (6) can be viewed as a representation of the variation of the ratio between the number of isotopes ^{14}C and the (more abundant) stable isotope of carbon, ^{12}C in the sample, $N(^{14}C)/N(^{12}C)$. The ^{14}C atoms form a very small fraction (vide infra) of the carbon atoms so that the amount of ^{12}C atoms can be taken as constant. The activity of the carbon sample decays in the same way as the number of ^{14}C atoms [13] so that, after interrupting the ^{14}C exchange process, the $N(^{14}C)/N(^{12}C)$ ratio decreases continuously from the value existing at the time of death of the organism. Accordingly, the ratio of radiocarbon to stable carbon will reduce according to the exponential decay law:

$$\frac{N(^{14}C)}{N(^{12}C)} = \left(\frac{N(^{14}C)}{N(^{12}C)}\right)_{\text{living organism}} \exp(-\lambda t) \quad (8)$$

t being the amount of time that has passed since the death of the organism. Then, that time can be calculated if the $N(^{14}C)/N(^{12}C)$ ratio is determined upon assuming that the corresponding ratio for the living organism was the same as the mean ratio in the biosphere, approximately, 1.5 parts of ^{14}C to 10^{12} parts of ^{12}C (including ca. 1 % of carbon atoms of the other stable isotope, ^{13}C).

Originally, what was measured was the activity of the samples; i.e., the number of disintegration events per unit mass and time, using a Geiger counter. As the measured activity is representative of the number of ^{14}C atoms in the sample, there is need of performing counting measurements during relatively long times for accumulating a reasonably high number of counts. Further developments resulted in the use of gas proportional counters, liquid scintillation counters (beta counters) and accelerator mass spectrometry (AMS) [14]. This last technique measures the 'quiet' ^{14}C atoms and not only those experiencing disintegrations so that it is intrinsically more sensitive than conventional radioactivity measurements. The problem is, however, the superposition of the signals for ^{14}C and ^{14}N atoms. Filtering with a gold foil can be used for solving this problem.

Radiocarbon dating can be applied to most organic materials and spans dates from a few hundred years ago right back to about 50,000 years ago but for dating to be possible, the material must once have been part of a living organism. This means that stone, metal and pottery can only be dated by this method if there is some organic material embedded or left as a residue.

Samples for dating have to be treated to convert it into a suitable form (gaseous, liquid, or solid), depending on the measurement technique to be used. Pretreatments are needed to remove any contamination and spurious constituents. For instance, alkali and acid washes are used to remove humic acid and carbonate contaminations. The size of the sample is also a factor to be accounted; for Geiger and beta counters, a sample weighing at least 10 g is typically required. AMS methodology generally requires less than a gram of most sample materials [15].

Complete wood samples can be analyzed, as well as only the cellulose fraction. Unburnt bone can be dated by analyzing collagen, the protein fraction that remains after washing away the bone's structural material. For bones burnt under reducing conditions, there is also possibility of dating because of carbonization of the organic matter. Shells from both marine and land organisms consisting of calcium carbonate can be also analyzed. Conchiolin, a protein existing in shell, can also be used for dating purposes.

Figure 6 shows the activity vs. time from data originally provided by Libby and Arnold [10] for testing the possibility of radiocarbon age determination. Calibration was performed from samples of wood from several tombs of Egyptian pharaohs

Problems of radiocarbon dating

There are several problems to be considered:

(a) Reservoir effects: As previously indicated, there is a continuous exchange of ^{14}C, generated by the cosmic rays in the atmosphere, between different Earth systems constituting reservoirs of the element. The deep ocean contains the majority (90.8 %) of the Earth carbon, and the remaining carbon is distributed between the surface oceans (2.4 %), the atmosphere (1.9 %), the terrestrial biosphere (1.3 %) and the dead organic matter (3.6 %). The $^{14}C/^{12}C$ ratio, however, differs from one reservoir to another. Thus, it has been estimated that the time taken for carbon

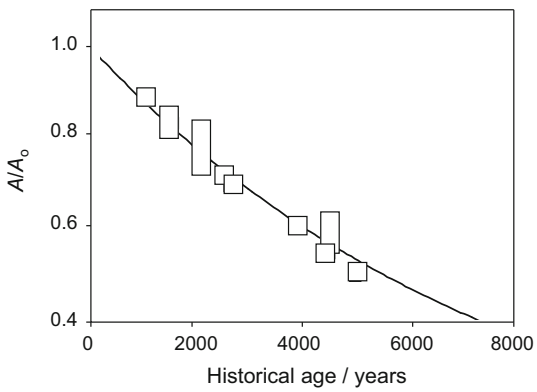

Fig. 6 ^{14}C activity ratio between the ancient samples and the modern activity vs. historical age curve adapted from the "Curve of Knowns" after Arnold and Libby [12] using samples of known age primarily from Egypt. The theoretical curve was constructed using the half-life of 5,568 years

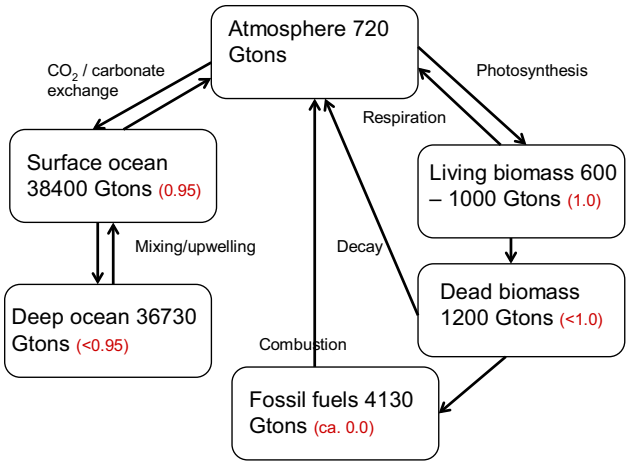

Fig. 7 Simplified view of the terrestrial carbon reservoirs. Estimated amounts in Giga tons and $^{14}C/^{12}C$ ratio relative to the atmospheric $^{14}C/^{12}C$ ratio (numbers in red). Adapted from [15] and [17]

of the atmosphere to mix with the carbon of oceans surface is only a few years whereas it takes about 1,000 years to circulate the water between the lowest and highest layers of the ocean [16, 17]. As a result, the $^{14}C/^{12}C$ ratio in each reservoir slightly differs from the atmospheric ratio (see Fig. 7 where the values of the $^{14}C/^{12}C$ ratio of different reservoirs relative to the atmospheric $^{14}C/^{12}C$ ratio are provided).

(b) Variation in the atmospheric $^{14}C/^{12}C$ ratio: This effect, also called de Vries[8] effect, consists in the 'historical' variation of the atmospheric $^{14}C/^{12}C$ ratio. This was established by testing wood samples of known ages and confirmed by correlating radiocarbon ages with overlapping series of tree rings forming a continuous sequence of tree-ring data allowing to estimate the atmospheric $^{14}C/^{12}C$ ratio at a given age from the $^{14}C/^{12}C$ ratio at the tree ring of known age. Due to the significant longevity of such species, the first calibrations were performed from wood samples obtained from the giant California sequoia (*Sequoia gigantea*), the European oaks (*Quercus* spp.), and, for the oldest portions of the time series, the bristlecone pine (*Pinus longaeva*), further extended to a time interval of 9,800 years [17, 18].

(c) Anthropogenic effects: Correspond to the variations in the atmospheric $^{14}C/^{12}C$ ratio associated with the human activity. The first affect is associated with atmospheric nuclear testing occurring from about 1950 until 1963, and consists of an increase in the atmospheric $^{14}C/^{12}C$ ratio with a maximum in 1965. The second effect, also known as Suess[9] effect, results from the extensive burning of coal and oil since the industrial revolution in the 1800s. Fossil combustibles contain rather small amounts of ^{14}C because they are very old [19].

(d) Isotope fractionation: Photosynthesis is the primary process by which the living organisms incorporate carbon. In this process, ^{12}C is absorbed more easily than ^{13}C which in turn is more easily absorbed than ^{14}C. As a result, the $^{14}C/^{12}C$ ratio in plants (and subsequently in the animals) differs from the $^{14}C/^{12}C$ ratio in the contemporary atmosphere. As far as isotope fractionation varies from one species to another, the common practice is to evaluate it for each sample that is dated. For this purpose, the carbon-13 concentration is measured because this is a stable isotope (present at about 1 % in natural carbon) and that concentration can be determined using an ordinary mass spectrometer. Table 2 summarizes the isotopic fractionation in different materials [18]. In this table, $\delta^{13}C$ is the difference (expressed in parts per thousand) between the $^{13}C/^{12}C$ ratio in the sample to the ratio for the Pee Dee Belemite carbonate standard (PDB):

$$\delta^{13}(\mathrm{C}) = \left[\frac{\left(\frac{N(^{13}\mathrm{C})}{N(^{12}\mathrm{C})}\right)_{\text{sample}}}{\left(\frac{N(^{13}\mathrm{C})}{N(^{12}\mathrm{C})}\right)_{\text{PDE}}} - 1 \right] \times 1{,}000 \qquad (9)$$

In the case of marine organisms, the isotope fractionation effect depends significantly on temperature because the solubility of CO_2 in water decreases when increasing temperature. The carbon exchange between atmospheric CO_2 and carbonate at the ocean surface is also subject to fractionation, resulting in an increase in the $^{14}C/^{12}C$ ratio in the ocean of ca. 1.5 %, relative to the $^{14}C/^{12}C$ ratio in the atmosphere. This effect, however, is compensated by the decrease in the $^{14}C/^{12}C$ ratio caused by the upwelling of water from the deep oceanic regions which contain 'old' carbon. This means that the residence time, i.e., the average time spent by a carbon atom in a given reservoir before returning to the atmosphere, and the rate at which the mixing or exchange of carbon-14 atoms between two

[8] The effect was found by Hessel de Vries (November 1916–December 1959), a Dutch physicist who has greatest merits in the development of radiocarbon dating, and many believe that he would have shared the Nobel prize with Libby, if he would not have committed suicide in 1959, after he has murdered his female assistant when she did not return his affection [see Engels JJM (2002) Vries, Hessel de (1916–1959). In: Biografisch Woordenboek van Nederland. Den Haag].

[9] Hans Eduard Suess (16 December 1909–20 September 1993) Austrian born American physical chemist and nuclear physicist, who discovered the effect of fossil fuel burning on the $^{14}C/^{13}C$ ratio.

Table 2 Typical $\delta^{13}C$ values for different substrates for radiocarbon dating [18]

Material	$\delta^{13}C$ (‰)
Wood, charcoal, peat	-25 ± 3
Bone collagen, aminoacids	-20 ± 2
Freshwater plants	-16 ± 2
Bone apatite	-10 ± 2
Atmospheric CO_2	-9 ± 2
Non-marine carbonates	-5 ± 5
Marine carbonates	0 ± 3

systems occurs influence the age estimate. For instance, the apparent age of the radiocarbon from the deep ocean is about 400 years. Similarly, a significant part of the dissolved carbon in river water comes from the dissolution of 'old' calcareous rocks so that the carbon in such water has an apparent age of several thousand years or more.

(e) Half-life correction: The currently accepted value for the ^{14}C half-life, 5,730 years, differs from the originally measured by Lobby, 5,568 years. To maintain the calculations prior to 1960, the original half-life is still used in calculations expressing times in 'radiocarbon years', subsequently correcting it.

(f) Hemisphere effects: The atmospheric $^{14}C/^{12}C$ ratio in the northern hemisphere is larger than in the southern hemisphere. This is probably because of the greater surface area of the oceans on the southern hemisphere so that there is more carbon exchanged between the ocean and the atmosphere than on the northern hemisphere and the atmospheric circulation systems are independent enough to prevent equilibration.

(g) Geophysical effects: Geomagnetic effect: the cosmic ray particles which produce the neutrons for the reaction of formation of carbon-14 are electrically charged and, consequently, they are deflected by the Earth's magnetic field. Variations of the geomagnetic field with time and with the location result in fluctuations in the ^{14}C production. In particular, the processes of geomagnetic reversal involve periods of time of several 1,000 years where the strength of the Earth magnetic field falls to a rather low value and then the carbon-14 production is enhanced. Roughly, a 20 % of increase in the average strength of the geomagnetic field causes a 10 % decrease in the production of ^{14}C.

The above effects are superimposed to the heliomagnetic modulation of the magnetic field. Sunspot activity intensifies the weak interplanetary magnetic field so that the fluctuations of solar activity (with long-time and short-time components) influence the production of carbon-14 in the Earth.

(h) Geochemical effects: There are several effects associated with geological processes:

Volcano effect: Volcanic eruptions eject significant amounts of carbon (as carbon dioxide) of ancient geological origin (i.e., with no traces of ^{14}C) to the atmosphere so that the $^{14}C/^{12}C$ ratio is depressed in the region of influence of the eruption.

Hard water effect: Appearing as a result of the pass of carbonate ions to waters permeating calcareous rocks. Since these rocks are usually 'old', they contain low or even non-measurable amounts of ^{14}C, thus lowering the $^{14}C/^{12}C$ ratio of the waters.

Humic acids effect: Other sources of carbon such as humic substances (humic acids, fulvic acids, all components of peat, etc.) all contain 'old' carbon, thus resulting in the lowering of the $^{14}C/^{12}C$ ratio.

Radiocarbon ages; calibration and errors

As explained below, the radiocarbon date tells us when the organism was alive (not when the material was used). This fact should always be remembered when using radiocarbon dates. The dating process is always designed in such way as to extract the carbon from a sample which is the most representative of the original organism. In general, it is always better to date a properly identified single entity (such as a cereal grain or an identified bone) rather than a mixture of unidentified organic remains.

Standard ^{14}C-based age estimates are expressed in terms of a set of parameters that define the so-called conventional radiocarbon age, introduced by Stuiver and Polach [20, 21]. These include: (1) using Libby's ^{14}C half-life (5,568 years) rather than the currently accepted value ($5{,}730 \pm 40$ years); (2) using AD 1950 as the zero point from which to count time; (3) the normalization of the measured ^{14}C concentration to a common $^{13}C/^{12}C$ ($^{13}\delta$) value to correct for natural fractionation effects; (4) assuming that the concentration of ^{14}C in all reservoirs has remained constant over the entire ^{14}C time scale. Traditionally, ages are expressed in calendar years with respect to the birth of Jesus Christ (by adding AD (anno domini) or BC (before Christ)). In radiocarbon dating, BP means 'years before present' which is defined as AD 1950. The 1985 International Radiocarbon Conference at Trondheim recommended the use of cal AD, cal BC and cal BP for calibrated ages using radiocarbon years. Figure 8 compares the envelopes of standard deviation for the calibration

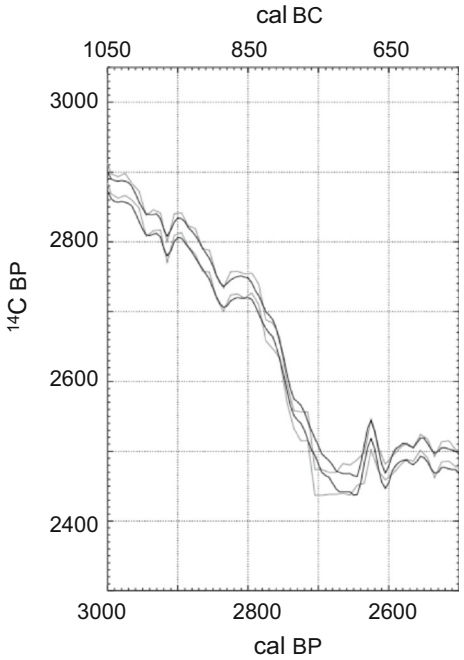

Fig. 8 Comparison of IntCal98 (*gray lines*) and IntCal04 (*black lines*) standard deviation error envelopes for radiocarbon dating in the range 2,500–3,000 cal BP. From Ref. [22], with permission

curves for radiocarbon dating in the period 2,500–3,000 cal BP using the calibrations IntCal98 (gray lines) and IntCal04 (black lines) [22, 23]. These calibrations account for the different factors mentioned in "Problems of radiocarbon dating" so that the calibration graph differs markedly from a monotonically increasing or decreasing curve.

The age in conventional radiocarbon years before AD 1950 is given by:

$$\text{Age} = 8{,}033 \ln\left(\frac{A}{A_{\text{m}}}\right) \tag{10}$$

where A is the activity of the sample corrected for isotope fractionation effect and A_{m} the standard modern activity.

There are, however, additional deviations to be accounted so that ages calculated from Eq. (9) should be corrected. The uncertainty in the measured age, Δt, can be evaluated again using the conventional theory of error propagation (see "Appendix 1") so that:

$$\Delta t = \left(\frac{\Delta\lambda}{\lambda}\right) t + \frac{1}{\lambda}\left(\frac{\Delta A}{A}\right) + \frac{1}{\lambda}\left(\frac{\Delta A_{\text{m}}}{A_{\text{m}}}\right) \tag{11}$$

In the above equation, $\left(\frac{\Delta\lambda}{\lambda}\right)$ represents the relative uncertainty in the radioactive constant (ca. 0.8 % in the case of radiocarbon), estimated from calibration data, and $\left(\frac{\Delta A_{\text{m}}}{A_{\text{m}}}\right)$ and $\left(\frac{\Delta A}{A}\right)$ the relative uncertainties of A_{m} and A, respectively, those quantities reflecting the statistical precision of the corresponding measurements. Equation (11) indicates that, providing that these two last relative uncertainties remain constant, the uncertainty in the age increases with the age of the sample.

In radiocarbon dating, the uncertainty is strongly dependent on the type and size of the sample and the experimental method. In the case of conventional beta-counting in radiocarbon dating, a duration of 1 day is needed for counting a sufficient number of disintegrations to reach a statistical precision of ±0.5 % using a sample of several grams of total carbon. It is pertinent to note that that this counting statistics does not represent all the uncertainties in radiocarbon dating and that the errors resulting from type of sample, preparation and laboratory differences are difficult to estimate. Under these circumstances, the standard deviation (SD) associated with the statistical precision cannot be considered as a suitable estimate of the 'real' error in the dating. Accordingly, the SD is multiplied by a numerical factor, called error multiplier, providing an increased, more realistic SD based on the consideration of different factors of the error, as discussed in detail in literature [21]. As previously noted, the time required for performing measurements yielding a reasonable uncertainty depends on the amount of sample and the counting technique. This is crucial in cases such as the Shroud of Turin (see "Appendix 2"). The introduction of the AMS methodology has permitted to lower the amount of sample from at least 10 g to less than a gram [15].

Other cosmogenic radioisotopes

Other cosmogenic radioisotopes produced in the Earth by cosmic rays can in principle be used for dating purposes and geological studies (see Table 3). Early proposals were made by Davis and Schaffer [24] and Fröhlich and Lübert [25]. Several radioisotopes were formed before the condensation of the solar system by the process of cosmic ray spallation on interstellar gas and dust so that their use for dating purposes would require complicated corrections [26–29]. Figure 9 shows a simplified scheme for the formation of cosmogenic isotopes.

The optimal demands for dating purposes are: (1) having a geologically or archeologically relevant value of the isotope half-life; (2) extensive and preferentially uniform distribution in the biosphere and/or geological strata; (3) production exclusively by means of a cosmogenic process; (4) production at constant rate; (5) suitability of radioactivity measurement; (6) existence of a well-defined event for defining the time zero; (7) limited incidence of attenuation, etc. processes. Although activity measurements are available to AMS techniques, there are several problems, namely, the uncertainty about the initial activity at time zero, absence of world-wide exchange reservoirs and important local fluctuations. The case of calcium-41 is paradigmatic: ^{41}Ca is formed in the soil as a result of the

Table 3 Half-lives of some cosmogenic radioisotopes

Isotope	Half-life (thousands of years)	Formation reaction	Application
^{26}Al	720	^{28}Si(n,p2n)^{26}Al	Dating of rocks and meteorites
^{10}Be	1,600	^{16}O(n,4p3n)^{10}Be	Sedimentation rates
^{41}Ca	103	^{40}Ca(n,γ)^{41}Ca	Dating of carbonate rocks
^{36}Cl	308	^{35}Cl(n,γ)^{36}Cl	Dating of rocks, groundwater tracer
^{129}I	15,700	^{129}Xe(n,p)^{129}I	Groundwater tracer

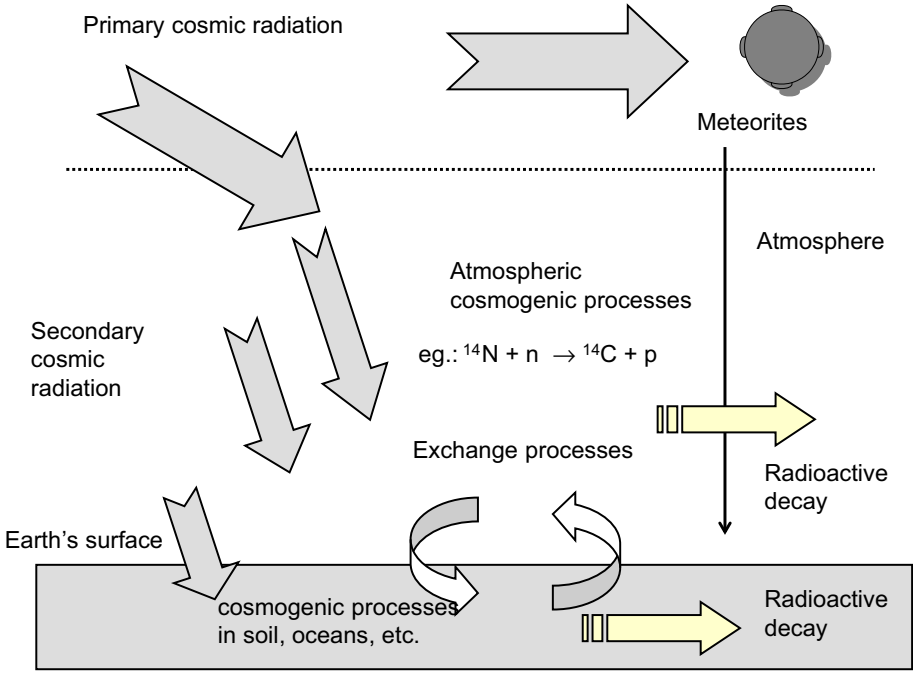

Fig. 9 Schematic representation of the main processes involved in the formation of cosmogenic isotopes

action of neutrons on ^{40}Ca, but because neutrons are attenuated in soil, this process occurs only in the top 1 m. Below a depth of 3 m, the process completely stops.

The dating method may involve the measurement of the relative abundance of the daughter isotopes. This is the case of ^{26}Al and ^{10}Be; such isotopes are produced under the action of cosmic rays in quartz crystals in the Earth's surface at a ratio of ^{26}Al:^{10}Be = 6.75:1 [30]. If the quartz crystal is further buried below the penetration depth of cosmic rays, the production of the isotopes stops and both nuclides decay at different rate so that the ^{26}Al/^{10}Be ratio decreases over time and can be used to date the burial event.

This case can be treated such as competing reactions in chemical kinetics where a parent reagent A gives rise to two products B and C by means of competitive processes. The kinetic equations for first-order kinetics are:

$$\frac{dc_A}{dt} = -\lambda_B c_A - \lambda_C c_A; \quad \frac{dc_B}{dt} = \lambda_B c_A; \quad \frac{dc_C}{dt} = \lambda_C c_A \tag{12}$$

where c_A, c_B, c_C, represent the respective concentrations of A, B and C, and λ_B and λ_C are the rate constants for the A → B and A → C reactions. The relevant point to emphasize is that, at sufficiently long time, the concentrations of the daughter products B and C become constant:

$$\frac{c_C}{c_B} = \frac{\lambda_C}{\lambda_B} \tag{13}$$

Accordingly, the uncertainty in age estimates is related, among other factors, to that of the decay constant. Figure 10 compares the calibration data for dating buried quartz using various pairs of cosmogenic nuclides [30]. The theoretical uncertainties (lines) depicted here correspond to those associated with decay constant uncertainties following a treatment such as discussed in "Appendix 1".

Apart from radioactive cosmogenic isotopes, there are stable cosmogenic isotopes, in particular, ^{3}He and ^{21}Ne which are formed in olivine, quartz and other minerals by the action of cosmic rays. Then, the rate of production of such isotopes fits to a linear law:

$$c_0 = P_0 t \tag{14}$$

where c_0 denotes the concentration at the Earth's surface and P_0 the rate of production at the surface, whereas the

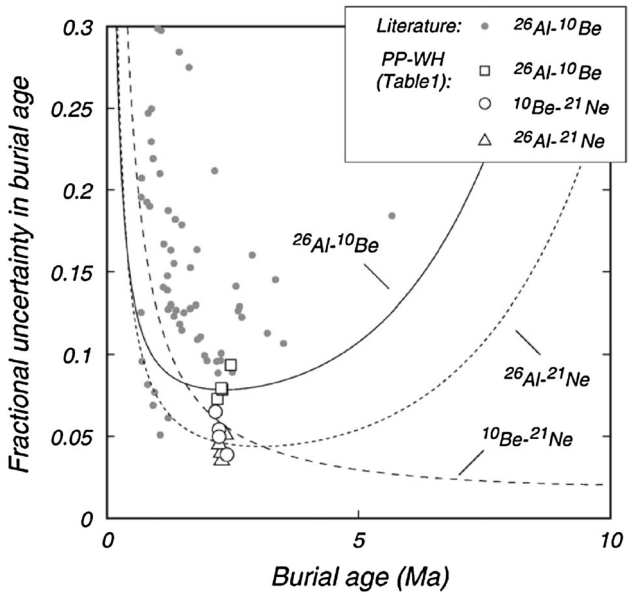

Fig. 10 Uncertainty analysis for dating buried quartz using various pairs of cosmogenic nuclides. Uncertainties depicted here are the 'total uncertainty' or the 'external uncertainty' of various authors and reflect measurement and decay constant uncertainties. From Ref. [30] with permission

rate of production of radionuclides such as ^{10}Be can be expressed as:

$$c_0 = \frac{P_0}{\lambda(1 - e^{-\lambda t})} \quad (15)$$

Stable cosmogenic isotopes are of interest for dating because of their stability, thus prompting for longtime measurements. Assuming that the stable nuclide is cosmogenic and is predominantly produced by a single mechanism (typically, neutron spallation), then the concentration c at a depth z will be given by [31]:

$$c = c_0 \exp\left(-\frac{\rho z}{\Lambda}\right) \quad (16)$$

where Λ is the attenuation length scale of cosmogenic production and ρ is rock density. There is need to consider several corrections, in particular, erosion effects and the contribution of non-cosmogenic sources; for instance, non-cosmogenic ^{3}He is commonly found in minerals either from the reaction ^{6}Li(n,α)^{3}H $\rightarrow$ ^{3}He or from the presence of mantle helium in fluid inclusions [32].

Dating extraterrestrial matter

Dating meteorites and other extraterrestrial matter can be performed using isotopes generated by the interaction of target nuclides of the object with galactic cosmic rays (mainly consisting of protons and other atomic nuclei). These rays originate from outside our solar system and constitute the most energetic particles in the interplanetary space. Their distribution is isotropous and their omnidirectional flux at 1 astronomical unit of distance is about 3 particles cm^{-2} s^{-1} for particles having kinetic energy larger than 1 GeV particle^{-1}.

For dating purposes, measurements of the concentration of either stable and/or radioactive cosmogenic nuclides can be used. As basic assumptions are taken: (1) the flux of primary cosmic rays was constant in time and constant in space; (2) the shape and chemical composition of the sample did not change appreciably, (3) any cosmogenic contributions from prior periods of irradiation and all non-cosmogenic contributions to the inventory of the nuclide of interest are known, and (4) the sample did not lose nuclides of interest except by known rates of radioactive decay. The cosmic ray exposure ages are mainly calculated from the ^{83}Kr/^{81}Kr, ^{36}Ar/^{36}Cl and ^{41}K/^{40}K ratios [33].

A case of particular interest was the Allende meteorite, which fell in the north of Mexico (near the village of Pueblito de Allende) on 8 February 1969. The proportion of ^{26}Mg (one of the stable isotopes of magnesium) measured in inclusions in the meteorite (11.5 %) was higher than its normal abundance. This excess of magnesium suggested that the radioactive ^{26}Al whose disintegration is responsible for the appearance of ^{26}Mg was incorporated into the meteorite less than a few million years after its creation. As far as ^{26}Al is formed by thermonuclear reactions in the interior of stars, the most reasonable hypothesis for explaining the presence of this 'young' magnesium was that a supernova exploded just before the birth of the Solar System and perhaps this event influenced decisively the composition of the same. It is generally accepted, however, that the supernova event was not particularly influential on the origin of the Solar System [34].

The oxygen isotope time scale

The main isotope of oxygen, ^{16}O, is accompanied by two other stable isotopes, ^{17}O and ^{18}O. The ratio between the different oxygen isotopes is not the same in all systems because several geological and biological processes occur with relative enrichment of one of them. The variation of the isotopic composition associated with such processes is termed isotopic fractionation. Neglecting the contribution of ^{17}O, much less abundant than the other isotopes, the isotopic fractionation relative to a given standard (usually the so-called standard mean ocean water, SMOW) is defined as:

$$\delta^{18}O = \frac{(^{18}O/^{16}O) - (^{18}O/^{16}O)_{standard}}{(^{18}O/^{16}O)_{standard}} \times 1{,}000 \quad (17)$$

where δ^{18}O is given usually as a fraction per thousand (‰).

Fractionation takes place in the case of water evaporation, since $H_2^{16}O$ is more volatile than $H_2^{18}O$. As a result,

rainwater is ^{16}O enriched and the surface ocean contains greater amounts of ^{18}O around the subtropics and tropics where there is more intense evaporation than in the mid-latitudes. This means that, during the glaciations, where a large amount of water was locked up in glacial ice (enriched in ^{16}O), the remaining sea water was enriched in ^{18}O. Such variations in the isotopic composition are in turn reflected in the $^{18}O/^{16}O$ ratio in the shells of marine organisms such as foraminifera. Temperature and salinity influence oxygen isotope fractionation so that $\delta^{18}O$ provides information of high paleoclimatic value. Roughly, there is a decrease in $\delta^{18}O$ of 1 % by each 4.2 K increase in water temperature.

The variations in the $^{18}O/^{16}O$ ratio can be measured with a high-precision mass spectrometer from ice cores extracted from polar ice caps as well as in shells in deep sea sediments. The idea that the isotopic composition of natural systems is temperature-dependent was anticipated by Urey [35][10] and the first result from the shells of planktonic foraminifera in a core of sea-bottom sediment was reported by Emiliani [36]. Such data provide relevant information which is frequently combined with paleomagnetic data and different dating techniques (radiocarbon, potassium–argon) in paleoclimatic studies.

Alternatively (or complementarily), dating from oxygen isotope fractionation can be obtained from estimates of the sedimentation rate. Correlation of marine paleoclimate with continental one can be obtained crossing data from marine sediments with, among others, pollen series in continental (and marine) sediments.

The isotope fractionation phenomena also occur for other elements and δ quantities can be defined using formulas similar to that in Eq. (17) upon defining appropriate standards. For instance, carbon isotope ratios are defined relative to Pee Dee Belemite carbonate (PDB), whereas nitrogen isotope ratios are defined relative to atmospheric nitrogen. Table 4 summarizes several representative isotope fractionation parameters.

More radiometric techniques

Uranium series dating

Radiometric dating techniques are based on the comparison of the amounts (concentrations) of two isotopes connected by a radioactive chain (see Fig. 11). The parent isotope has to be radioactive whereas the daughter isotope can be either radioactive (uranium–radium series, for instance) or stable (uranium–lead series). Uranium in nature is composed of two primordial radioactive isotopes, ^{235}U and ^{238}U, each one giving rise to a chain of daughter radioisotopes through successive processes of radioactive decay. As far as the activity of ^{238}U is ca. 22 times larger than that of ^{235}U, dating based on the former (major series) is more sensitive than dating based on the second (minor series); i.e., the major series permits using samples with much lower concentrations of uranium than the minor series.

For dating purposes, the unique relevant isotopes in such chains are those of long half-life, namely, ^{238}U (45,000 million years), ^{234}U (245,000 years), and ^{230}Th (75,400 years). As far as all these isotopes are radioactive and connected to a radioactive chain, it is assumed that a radioactive equilibrium is finally established and then the rate of decay of ^{230}Th equals its rate of production. Regarding ^{234}U decay to ^{230}Th (see Fig. 11), measurements of the $^{230}Th/^{234}U$ ratio can be used for dating events occurring at times before the establishment of the equilibrium of the corresponding radioactive series. Alpha spectrometry and mass spectrometry are the techniques used for measurements.

Uranium-based dating is typically applied to date karstic carbonate rocks because the crystals of calcite formed from ground waters contain trace levels of uranium but not of thorium (its carbonate salt is much more insoluble than uranium carbonate). Then, thorium is formed upon radioactive decay of uranium in the calcite crystals. The method is applicable, with limitations, to travertines, bone and dentine, coral and mollusk shells.

Potassium–argon and argon–argon dating

This method is based on the radioactive decay of potassium-40, the only naturally occurring radioactive isotope of potassium. This process yields argon-40 via electron capture (and also by positron decay) accompanied by γ emission. Argon is a gas whose accumulation, entrapped within potassium-bearing minerals, can be monitored in the gas released upon fusion of the sample by means of a mass spectrometer. Laser ablation permits to apply the technique to single crystal grains. In an earlier version of the technique, the potassium content was measured by atomic absorption spectrometry and other techniques, the decrease in the potassium content being representative of the $^{40}Ar/^{40}K$ ratio, and the quantity used for age estimates [37].

The potassium–argon method is usually applied to date metamorphic and igneous rocks. Here, the method provides the time passed since the mineral cooled below its closure temperature, which can be regarded as the temperature below which the mobile (easily diffusing or very fast annealing of disturbed crystal lattice) daughter isotope, resulting from the radioactive decay of a parent isotope,

[10] Harold Clayton Urey (April 1893–January 1981) American researcher which was awarded with the Nobel Prize in Chemistry in 1934 for their pioneering work on isotopes.

Table 4 Isotope fractionation parameters

Element	Isotope fractionation	Determined ratio	Standard	Absolute ratio
Oxygen	$\delta^{18}O$	$^{18}O/^{16}O$	SMOW, PDB	2.0052×10^{-3}
Oxygen	$\delta^{17}O$	$^{17}O/^{16}O$	SMOW	3.76×10^{-4}
Carbon	$\delta^{13}C$	$^{13}C/^{12}C$	PDB	1.122×10^{-2}
Nitrogen	$\delta^{15}N$	$^{15}N/^{14}N$	Atmosphere	3.613×10^{-3}
Sulfur	$\delta^{34}N$	$^{34}S/^{32}S$	CDT	4.43×10^{-2}
Chlorine	$\delta^{37}Cl$	$^{37}Cl/^{35}Cl$	Sea water	0.31978

For oxygen, two standards have been defined, the relationship between their isotope fractionations being: $\delta\,^{18}O_{PDB} = 1.03086\,\delta\,^{18}O_{SMOW} + 30.86$

SMOW standard mean ocean water, *PDB* Pee Dee Belemite carbonate standard (from *Belemnita Americana* of Pee Dee formation), *CDT* troilite in the Canyon Diablo iron meteorite

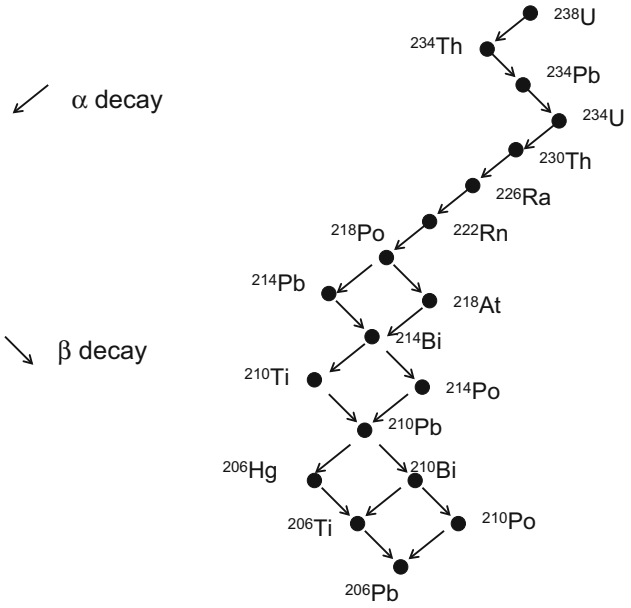

Fig. 11 Schemes for the uranium–radium series

becomes essentially immobile within the lattice of the mineral [38]. In the case of metamorphic rocks that have not exceeded their closure temperature, the age likely dates the crystallization of the mineral.

The radioactive decay of ^{40}K to ^{40}Ar is accompanied by the beta decay of ^{40}K to ^{40}Ca. Then, in a potassium-bearing system isolated from external influences, the growth of radiogenic ^{40}Ar and ^{40}Ca follows the equation:

$$[^{40}Ca] + [^{40}Ar] = [^{40}K](e^{\lambda t} - 1) \quad (18)$$

where the quantities in brackets represent the number of atoms at a given time. The overall radioactive constant, λ, is the sum of those for the decay to ^{40}Ar and ^{40}Ca (respectively, $0.581 \times 10^{-10}\ a^{-1}$, and $4.962 \times 10^{-10}\ a^{-1}$), $5.543 \times 10^{-10}\ a^{-1}$, corresponding to an half-life of 1,250 million years. The number of radiogenic ^{40}Ar atoms at a time t is:

$$[^{40}Ar] = \frac{\lambda_{EC}}{\lambda}\,[^{40}K](e^{\lambda t} - 1) \quad (19)$$

λ_{EC} being the radioactive constant for the ^{40}K to ^{40}Ar decay.

Assuming that the Ar was entrapped in the mineral soon after its crystallization, that none Ar was initially present in the mineral, and that none escaped during its geological history, the age of the mineral can be expressed as a function of the amount of accumulated radiogenic argon-40 as:

$$t = \frac{1}{\lambda}\ln\left(1 + \frac{\lambda}{\lambda_{EC}}\frac{[^{40}Ar]}{[^{40}K]}\right) \quad (20)$$

Additional assumptions must be made: that no excess ^{40}Ar was incorporated into the mineral during the crystallization and any subsequent metamorphic episodes; and that no additions or losses of potassium occurred during the geological history of the mineral with no occurrence of isotopic fractionation.

Corrections have to be made for the presence of atmospheric ^{40}Ar as well as for the excess of Ar occurring when the minerals were exposed to high partial pressure during an episode of regional metamorphism. This metamorphic veil effect can be estimated from $^{40}Ar/^{36}Ar$ and $^{40}K/^{36}Ar$ ratios.

The argon–argon method [39, 40] can be considered as a variant of the potassium–argon method in which the potassium content is monitored by the formation of argon-39 resulting from the neutron irradiation of potassium:

$$^{39}K + n = p + {}^{39}Ar \quad (21)$$

Argon-39 is radioactive, decaying by beta emission with a half-life of 269 years. The dating is based on the determination of the $^{40}Ar/^{39}Ar$ ratio by means of a mass spectrometer after neutron irradiation of the sample. Using this procedure, the $^{40}Ar/^{39}Ar$ ratio can be determined and compared with that of a mineral, the age of which is known irradiated by neutrons under identical conditions.

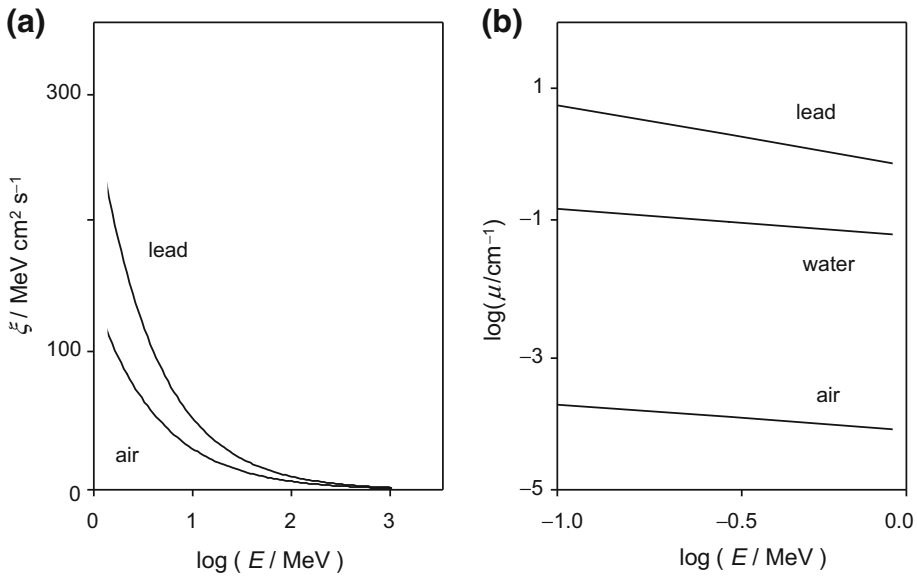

Fig. 12 Values of: **a** specific energy loss of ionization of protons moving through air and lead with different energies; **b** attenuation coefficient of γ rays of different energies in air, water and lead

The application of the argon–argon method involves as a first assumption that all argon-40 in the irradiated sample derives either from a radiogenic or an atmospheric origin, whereas argon-36 is of purely atmospheric origin and that all argon-39 is produced by the (n,p) reaction.

As in the case of the potassium–argon method, an atmospheric argon-40 correction has to be made. Additionally, interfering nuclear reactions such as $^{40}Ca(n,n\alpha)^{36}Ar$ and $^{36}Ar(n,\gamma)^{37}Ar$ have to be accounted for. A general problem, however, is the loss of argon-39 because of its recoil arising from the nuclear reaction described by Eq. (21). This effect is dependent on the size of the grains of mineral, because the loss of argon-39 from a potassium-bearing mineral grain may occur from a surface layer 0.08 mm thick. Then, the method cannot be applied to certain minerals, such as the glauconites, which comprise aggregates of crystals about a micrometer thick.

In spite of these limitations, the argon–argon method has several advantages over the potassium–argon one. The most relevant is that only ratios of argon isotopes have to be measured to calculate an age rather than absolute quantities so that there is no need of extracting all radiogenic argon from a mineral to derive an accurate age. A case study that was an extensive public divulgation is presented in the "Appendix 5".

Techniques based on nuclear radiation damage

General considerations

The term nuclear radiation is used here to designate the flux of nuclei, gamma radiation and subnuclear particles which can interact with the substances in the Earth's surface giving rise to processes of elastic and inelastic dispersion, excitation, and ionization. The intensity of such radiations decreases mainly due to the *bremsstrahlung* or free–free radiation effect and ionization effects produced in the matrix where it propagates. The effects of the nuclear radiation on solid substances are mainly two: (a) bond disruptions, resulting in lattice damage in crystals; (b) creation of electronic defects (trapped holes and electrons).

The attenuation of the nuclear radiations in atmosphere, soils, etc. is a factor of importance for dating because it varies significantly from one matrix to another. This can be seen in Fig. 12a where the specific energy loss of ionization, ξ, defined as the energy loss by thickness unit and density unit, of protons of different energies moving through air and lead are compared [41].

The attenuation of γ rays in a homogeneous matrix having a linear behavior can be expressed by the well-known Bouger–Lambert–Beer law [13]. Figure 12b shows the data for the linear attenuation coefficient of γ rays, μ, of different energies in air, water and lead, where important differences in the attenuation can be seen [42]. This is reflected in the different ionizing ability of such radiation in the different media, a crucial factor for several dating methods.

Fission track dating

There are several dating methods based on the cumulative damage exerted by nuclear radiations on crystal and glass structures. Thus, the radioactive alpha-decay of ^{238}U often occurs via fission yielding ^{234}Th and two α particles. These fission products have a large kinetic energy, and during their pass through the solid material, they leave a track of disruptions in the form of characteristic fission tracks of ca.

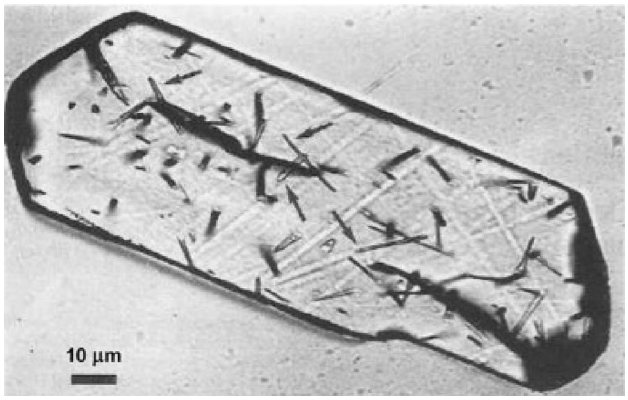

Fig. 13 An optical microscopy image of etched spontaneous tracks on a polished internal surface of apatite crystal. *Arrows* point to four individual confined tracks exhibiting original entire track lengths, which are useful for estimating the true length distribution. Taken from Ref. [46], with permission

0.01 mm length, visible under the microscope (see Fig. 13) after etching with an appropriate chemical reagent [43, 44]. The defects along the trails have higher reactivity and thus higher etching rate so that the fission tracks become marked and their counting can be made by optical microscopy (Fig. 13). Although such tracks can be observed in most minerals and glasses, only few of them are suitable for dating purposes, namely, apatite, mica and sphene. Apart from the above, the crystals of zircon and a volcanic glass, obsidian, are mostly used for dating. In the first case, sodium hydroxide is used for etching; for obsidian, hydrofluoric acid is used (with the necessary precautions).[11]

The age determination is then made from counting the number of tracks per unit of area in the sample relative to the extra tracks per area unit induced by exposure of the sample to the radiation of a nuclear reactor. This last quantity measures the ^{238}U content in the sample whereas the former quantity is representative of the spontaneous fission of ^{238}U during the 'history' of the sample. The ratio between these two quantities is proportional to the age of the sample but calibration using a standard of known age is usually made. Importantly, heating of the sample (above 800 °C for zircon) anneals the tracks, so that the 'clock' is re-initiated again when the sample is cooled. Again (see "Potassium–argon and argon–argon dating") the closure temperature plays an essential role in age determinations. Roughly speaking, this means that the ages calculated by this method correspond to the time interval since the sample was last heated (above the closure temperature).

Apart from fission tracks, energetic and heavy particles ($Z > 20$) from cosmic rays create permanent "latent" damage trails in silicates which can be directly observed by transmission electron microscopy (or can be chemically etched and enlarged to produce a conical hole that is visible by optical microscopy). The tracks in silicate grains are produced by nuclei from both solar and galactic cosmic rays, but these two sources of tracks can be distinguished from each other (see "Dating extraterrestrial matter"). The former produce with high track densities and track-density gradients at depth <0.1 cm, whereas the later can penetrate solid matter to depths of several centimeters [33, 45, 46].

Luminescence dating

The luminescence phenomenon consists of an emission of light made by some minerals upon thermal (thermoluminescence) or radiative (optically stimulated luminescence) excitation. Such processes can be associated with radiative quantum transitions experienced by trap or defect states generated as a result of the effect of ionizing radiations on the crystal of electronic insulators produced by traces of radioactive elements in the same and external radioactivity and cosmic rays. In the case of thermoluminescence, heating the material at a high enough temperature enables such trapped states to interact with the lattice vibrations (phonons) of the crystal structure, then decaying into lower-energy states with emission of photons.

It is pertinent to note that thermoluminescence appears upon heating between 100 and 500 °C, but there are other light emissions to be discriminated, the red-hot glow, corresponding to an incandescence emission at higher temperatures and spurious thermoluminescence associated with a variety of non-age-dependent causes. Importantly, precautions against sample exposure to light are needed, because a slow decrease in the thermoluminescent effect appears.

In the most simple case, schematically depicted in Fig. 14, the ionizing radiation produces in the ionic crystal a hole-electron pair localized in the valence and conduction bands, respectively. These can be trapped into available defect states associated with impurities, vacancies, interstitial ions, etc. in the lattice, avoiding the hole-electron recombination, as depicted in Fig. 14a. Upon heating, the thermal vibrations of the crystal provide sufficient energy to cause the release of the electron and a follow-up hole-electron recombination with concomitant emission of a photon (Fig. 14b). This process competes with undesired processes such as the non-radiative hole-pair recombination through other trap levels (Fig. 14c).

[11] HF has to be handled with extreme caution. See Peters D, Miethchen R (1996) Symtoms and treatment of hydrogen fluoride injuries. J Fluor Chem 79:161–165 and Ohtani M, Nishida N, Chiba T, Muto H, Yoshioka N (2007) Pathological demonstration of rapid involvement into the subcutaneous tissue in a case of fatal hydrofluoric acid burns. Forensic Sci Int 167:45–52.

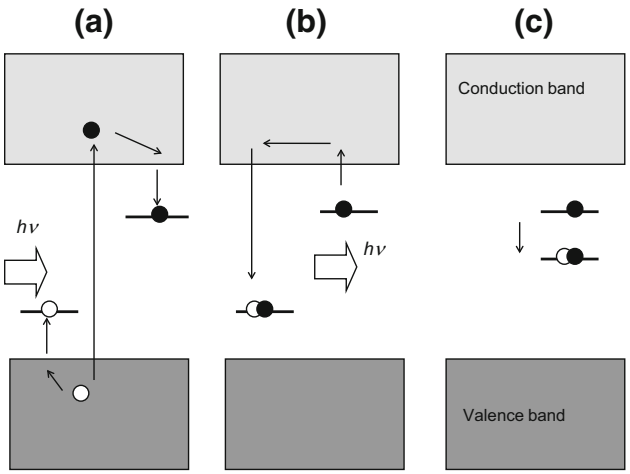

Fig. 14 Energy-level diagram for an ionic solid experiencing a thermoluminescence process. **a** hole-electron pair separation due to radiation excitation and storage in trap levels; **b** hole-electron recombination induced by lattice vibrations and thermoluminescent emission of light; **c** 'poisoning' effect of hole-electron non-radiative recombination using additional trap levels of impurities, vacancies, etc.

The thermoluminescence is typically observed in quartz and feldspar crystals, and hence, in pottery. As previously noted, it is based on the cumulative formation of radiation defects produced by internal and external radioactive isotopes, and also by cosmic rays (if samples were not buried too deeply in the soil). Such radioactive isotopes are mainly those of uranium, thorium and potassium-40, all having long half-lives so that the flux of radiation can be considered as a constant over archeologically relevant periods of time. As in the case of fission tracks, heating eliminates the thermoluminescent effect, thereby setting the 'clock' to zero. By obvious reasons, this is particularly useful for dating ceramic materials submitted to heating during the production process. Among other corrections, it has to be accounted the effect of induced fission associated with uranium-235.

The age is calculated from the archeological (or accumulated dose) thermoluminescence dose and the annual dose rate (for alpha, beta, gamma and cosmic radiation). The annual dose rate is usually determined by chemical and/or radiometric analysis of the sample and the surrounding sediments as well as by use of dosimeters, yielding the annual dose, and the sensitivity of the mineral in acquiring thermoluminescence, the thermoluminescence per dose unit. The sensitivity is determined upon exposition of portions of the sample to the radiation from a calibrated radioisotope source. Then, the age will be:

$$t = \frac{\text{Paleodose}}{(\text{Annual dose}) \times (\text{TL per unit dose})} = \frac{\text{Paleodose}}{\text{Annual dose rate}} \quad (22)$$

The accumulated dose is usually determined using the additive radiation technique [43].

It has to be taken into account that, in the case of pottery, the thermoluminescence is mainly produced by the nuclear reactions of potassium, thorium and uranium, but rubidium and the cosmic radiation also contribute to this effect. The irradiation dose is defined in terms of the ionizing effect produced in the air [47].[12] The units used for expressing the accumulated dose and annual dose rate are, respectively, Gy and Gy/a.[13]

Alpha, beta and gamma emissions from the material under study and also its surrounding soil in the usual case of buried pottery are involved in the measurements. Accordingly, the Eq. (22) needs to be modified as follows:

$$t = \frac{\text{Paleodose}}{D_\alpha + D_\beta + D_\gamma + D_c} \quad (23)$$

where D_α and D_β are the annual dose rate contributions of alpha and beta radiations (mainly 'internal'). In this equation, D_γ and D_c represent the annual dose rate contributions of the radiation gamma (mainly providing from the environment of the sample) and cosmic radiation, respectively. Obviously, estimation of such contributions requires detailed case-sensitive calibration experiments.

The optically stimulated luminescence (or photo-stimulated luminescence) is based on the stimulation by a xenon lamp or a laser source of the luminescent emission of minerals (quartz, feldspar, zircon). As in the case of thermoluminescence, but more drastically than in that case, the exposure of the mineral to sunlight reduces the emission, thus producing a resetting mechanism. Accordingly, only last exposure of the sample to the sunlight is datable. Other directly related methods are the optically stimulated phosphorescence and the phototransferred luminescence.

Electron spin resonance

This dating method is based, similarly to the above, on the measurement of the accumulated dose of nuclear radiation defects, now using the electron spin resonance spectroscopy (or electron paramagnetic resonance) technique. This technique, widely used in chemistry, involves the

[12] The irradiation dose of X and γ rays is measured in roentgen; this is defined as the radiation dose for which 0.001293 g of air form ions whose total charge equals one electrostatic unit, equivalent to the generation of 2.083×10^9 pairs of monovalent ions per cm^3 of air under normal conditions. This quantity is equivalent to the transfer of 6.8×10^4 MeV of energy per cm^3 of air. For other ionizing radiations, the dose is measured in roentgen equivalent physical (rep), defined as the dose of ionizing radiation which produces an absorption of energy per gram of irradiated substance equal to the loss of energy produced in 1 g of air by a dose of 1 r of rays X or γ.

[13] The gray (Gy) is defined as the dose absorbed of ionizing radiations equivalent to the absorption of 1 J of ionizing energy by kg of irradiated material. The dose rate is usually expressed in Gy by year.

measurement of the radiation absorbed by paramagnetic centers in a magnetic field. Interestingly, this technique can be applied to samples from mollusks and coral shells, as well as to tooth enamel where thermoluminescence assays cannot be applied owing to decomposition on heating. Trapped electrons give electron spin resonance spectra because they are unpaired electrons, and hence paramagnetic centers. Unlike thermoluminescence, the electron spin resonance technique does not destroy the electron defects in the crystal during measurements, i.e., measurements can be repeated [48].

Chemical methods

General considerations

Chemical methods of dating are based on the variation of the chemical composition of a given system upon time. Ideally, these changes should have occurred uniformly during time regardless of the immediate environment of the material to be dated. In general, however, the above conditions are only partially accomplished. In most cases, the chemical composition of the system under study is quite sensitive to the fluctuations in the environmental conditions. A conceptually single case is that of acidity measured in polar ice caps, which can be measured conductometrically. The acidity of the oceans is directly related to the carbonate cycle. Volcanic eruptions and intense melting during summer months yield abrupt increases in the acidity [49]. Then, the variations of the acidity of polar ice cores reflect the variations of the oceanic temperature.

The obsidian method

Obsidian is a rhyolitic volcanic material[14] formed by the rapid cooling of silica-rich lava (containing >70 % wt silica). This material was used in prehistoric times as a raw material to manufacture arrows, knives, or other cutting tools. When a fresh surface of obsidian is exposed to air as a result of the tool manufacturing, it contains about 0.2 % wt of water. Upon exposition to the air, obsidian absorbs water and forms a narrow "band", "rim", or "rind" of hydrated obsidian which grows along time whereas the surface becomes water saturated (containing about 3.5 % wt of water).

The obsidian dating method, introduced by Friedman and Smith [50], is based on the measurement of the thickness of the hydrated layer using a microscope. To measure the thickness of the hydration rim, a small slice of material is cut from the artifact under study, being ground down to about 30 μm thickness and mounted on a petrographic slide for its examination under the microscope. Since the hydration layer is more dense than the unhydrated inside, there is an abrupt change in refractive index at the boundary that can be easily detected.

Assuming that the conditions of hydration remained uniform during the 'life' of the object, the thickness of the hydration layer is monotonically increasing with time. Interestingly, this hydration layer is very similar to the hydration layer of glass electrodes, which is responsible for their well-known pH sensitivity [51, 52]. Originally, the thickness x of the hydration layer was assumed to be proportional to the square root of time t, or, equivalently:

$$x^2 = kt \tag{24}$$

where k represents the water diffusivity (ideally equalizing the diffusion coefficient of water in the material) into the obsidian, which can be related to the Arrhenius expressions for the variation of diffusivity with the temperature [53]. This equation corresponds to diffusion under semi-infinite boundary conditions. Refinement of the method involves more detailed study of the diffusion. Figure 15 illustrates an image of the obsidian hydration rim in optical cross section [54].

Although this method provides the absolute age of the artifact, several factors complicate its effective application for this purpose. Thus, obsidian chemistry, including the intrinsic water content, affects the rate of hydration which is also influenced by temperature and water vapor pressure [55]. Accordingly, to use the obsidian method for absolute dating, the origin and hydration conditions of the sample have to be known and compared to samples of a known age [56, 57]. The re-use of the artifacts can also distort age measurements.

The hydration rate can be determined for a given archeological object through a measurement of the amount of intrinsic water via the direct infrared spectroscopic measurement, or by means of the determination of the density of the sample of volcanic glass.

The obsidian method has been recently expanded by the introduction of secondary ion mass spectrometry (SIMS) [58, 59] and infrared photoacoustic spectroscopy (IR-PAS) [54, 60]. Since a saturation layer is formed at the surface of the hydrated layer, the water content decreases with increasing depth. The SIMS method provides the in-depth profile of the distribution of hydrogen in the hydrated layer, thus obtaining the H_2O concentration versus depth profile. The most recent advance was the secondary ion mass spectrometry-surface saturation (SIMS-SS) method which involves modeling the hydrogen concentration profile and

[14] Rhyolites are silica-rich igneous rocks constituted by an assemblage of quartz, sanidine and plagioclase frequently including biotite and hornblende as accessory minerals.

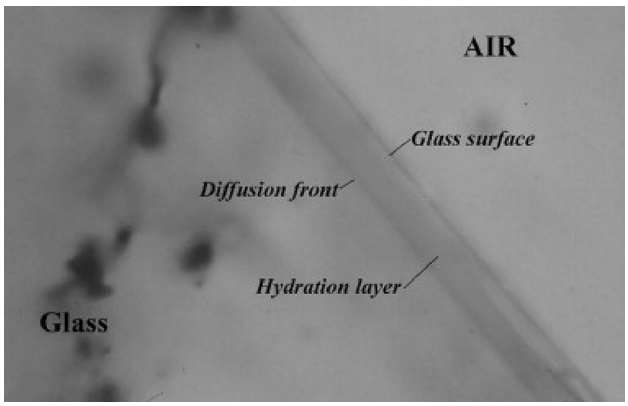

Fig. 15 Photograph of an obsidian hydration rim in optical cross-section. The hydration layer is approximately 10 μm thick. From Ref. [54], with permission

monitoring topographical effects by atomic force microscopy (AFM) [61, 62].

Aminoacid racemization

Racemization is the process in which one enantiomer (of D or L -or R and S- absolute configuration in chemical terminology) of an optically active compound spontaneously tends to convert to the other enantiomer. The optical activity is associated, in organic compounds, with the presence of asymmetric carbon atoms; those bound to four different groups in a tetrahedral arrangement. As a typical example, aspartic acid, whose structure is schematically depicted in Fig. 16. When there is only a single asymmetric carbon atom, there are two different forms, known as optical isomers or enantiomers, which are mirror images of each other, and cannot be superimposed with each other. The enantiomers, traditionally designated as D- and L-, display quite similar properties but differ in the angle of rotation of plane-polarized light.

In all known living systems, all amino acids in proteins (except glycine) possess at least one asymmetric carbon and, remarkably, all of them are L-amino acids. Once the L-form is incorporated to a living organism, it begins to racemize. The process is so slow; during the life of an organism, it is negligible but it is recognizable in organic materials at the scale of mega years. Then, the ratio between the D- and L-forms is representative of the age of the organic material. The degree of racemization can be measured using polarimetry, liquid chromatography, capillary electrophoresis, and mass spectrometry techniques. As a method of dating, aminoacid racemization was introduced by Bada et al. [63], based on previous reports of Hare, Mitterer and Abelson [64–66].

The rate of racemization depends on the type of amino acid and the average pH, temperature, humidity, and other characteristics of the enclosing matrix. It should be noted that low and high pH values increase notably the racemization rate. The technique can be used for dating fossil bones [67]. As a paradigmatic example, the racemization rate of aspartic acid was used for studying harpoon heads made of stone or ivory, probably used by Inupiat hunters in the late 1700s, encountered in bowhead whales that they have killed in the Beaufort Sea, southwest of the Arctic Ocean [68]. A number of applications have been described using this technique, from archeology [69] and paleontology [70] to forensic science [71]. In general, the racemization process follows a first-order kinetics which can be described by means of the equation:

$$\ln\left[\frac{1+(D/L)}{1-K(D/L)}\right] - \ln\left[\frac{1+(D/L)_o}{1-K(D/L)_o}\right] = (1+K)kt \quad (25)$$

where (D/L) represents the ratio of the concentrations of the D and L forms at a time t and $(D/L)_0$ the corresponding value at time zero. k denotes the racemization rate constant. K is a constant depending on the number of chiral centers.

Other chemical methods

Among others, one can mention the glass layer counting, consisting of the count of the weathering crusts leached out layers 0.5–20 μm sized appearing on archeological glasses. Determination of in-depth profiles of different elements (fluorine, uranium, nitrogen) by means of nuclear microprobes has been also used for dating purposes. The general idea is that, in contact with the environment, several elements leave (or enter) progressively the object modifying their original in-depth distribution. The concentration/depth profile varies with the age of the sample. Thus, the fluorine content in bones decreases rapidly with the depth for 'young' specimens, while it tends to be uniform for 'old' specimens.

Recently, it has been proposed a method for dating lead based on monitoring the extent of the corrosion process from measurement of the Meissner effect [72]. Above 7.2 K, lead metal exhibits diamagnetic susceptibility of the same order of magnitude as its salts and oxides. At temperatures below 7.2 K, the metal enters into the superconducting state acquiring a magnetic susceptibility 10^4–10^5 higher than that of its oxides and salts. In these circumstances, the determination of the volume magnetic susceptibility permits to calculate the mass of lead metal effectively existing in the sample and hence the mass of corrosion products in the same. Assuming uniform conditions of corrosion under burial conditions in carbonate-buffered soils, the growth of the mass per surface unit of the corrosion layer fits to a power law [72].

Dating metal objects is also possible, assuming that aging occurred under uniform conditions, by estimating the

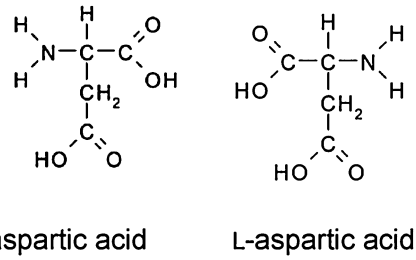

Fig. 16 Representation of the D- and L-enantiomers of aspartic acid

extent of the corrosion process from the record of characteristic electrochemical signatures of the compounds forming the primary and secondary patinas in lead [73, 74] and copper/bronze [75] artifacts. The proposed electrochemical methodology exploits the capabilities of the voltammetry of microparticles for the analysis of solid materials [76, 77]. This technique, which has been applied in archaeometry for authentication and tracing purposes [78], could be tentatively used for dating ceramics [79]. Figure 17 shows a voltammogram for a sub-microsample extracted from a bronze coin dated in 1,770 immersed into aqueous acetate buffer at pH 4.75. Here, the signals (I and II) for the reduction of cuprite (which forms the primary patina) and tenorite (forming in the secondary patina as a result of cuprite oxidation), respectively, are recorded. The tenorite/cuprite ratio increases with the corrosion time so that, in favorable cases, calibration data can be fitted to potential rate laws using the peak currents for the above signals. A relatively simple modeling [75] yields the following expression for the variation of the peak current ratio, $i_p(II)/i_p(I)$ on time:

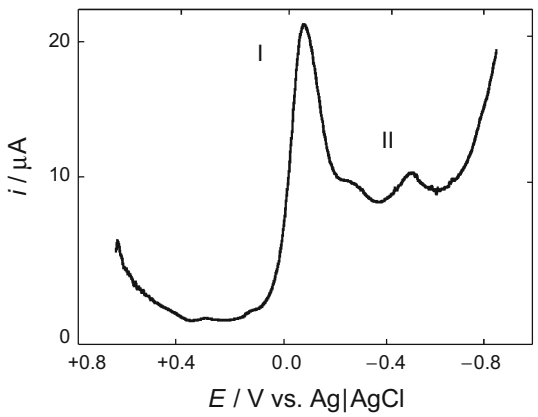

Fig. 17 Square wave voltammogram of a sub-microsample of a coin dated 1,770 attached to a paraffin-impregnated graphite electrode in contact with aqueous acetate buffer at pH 4.75. Potential scan initiated at +0.65 V in the negative direction; potential step increment 4 mV; square wave amplitude 25 mV; frequency 5 Hz. Peaks I and II correspond to the reduction of cuprite and tenorite, respectively

$$\frac{i_p(II)}{i_p(I)} \approx G + \frac{G_{II}}{G_I}\left[\frac{[(1+\beta)K_2 t]^{\frac{1}{1+\beta}}}{y_o^{1+\delta} + [(1+\delta)(K_1 - K_2)t]^{\frac{1}{1+\delta}}}\right] \quad (26)$$

where the G terms correspond to electrochemical constants to be determined upon calibration. K_1 and K_2 are rate constants for the growth of the primary and secondary patinas and β, δ the exponents of the corresponding potential rate laws. In the above equation, y_0 denotes the amount of primary patina by surface unit existing at the beginning of the process of formation of secondary patina.

The electrochemical methodology can also be applied for dating hemoglobin-containing archeological samples upon monitoring changes in the Fe(III)/Fe(II) iron couple and their catalytic enhancement in the presence of H_2O_2 [80].

Biochemical clocks

The so-called molecular clocks use the molecular changes associated with mutations to estimate the time passed since two species (or other taxonomical groups) diverged genetically. The molecular data used for such calculations are usually nucleotide sequences of DNA or amino acid sequences of proteins. The origin of such genetic clocks could be associated with the proposal of Zuckerkandl and Pauling [81] that the number of hemoglobin amino acid differences between different lineages changes roughly with time, as estimated from fossil evidence, and the notion of genetic equidistance introduced by Margoliash [82].

The key point, put forward by Kimura [83], assumes that there is a constant rate of mutations (strictly, 'neutral' mutations; i.e., those having no adaptive character) n occurring in a population of N individuals (assumed to be haploids). Then, there will be nN mutations in the population and the probability that this new mutation will become fixed in the population is of $1/N$. As a result, there are n new neutral mutations fixed in the next generation of the population as a whole. Such mutations accumulate, so that in successive generations the genetics of the population will increasingly diverge from the parent population.

The use of molecular clocks is constrained, however, by a series of factors [84]: (1) the influence of the generation time, because the rate of new mutations depends at least partly on the number of generations rather than the time; (2) the size of the population (genetic drift) affecting the number of effectively neutral mutations; (3) specific differences in metabolism, ecology, etc.; (4) possible change in the function of the studied molecular marker; (5) changes in the intensity of the "selection pressure". Accordingly, the use of molecular clocks requires the account of a series of conditioning factors [85–88].

Concluding remarks

Physical and chemical methods of dating play an essential role in archeology, geology, paleontology and related fields. These methods can be conceived as analytical methods submitted to the usual rules regarding accuracy and precision, sensitivity, selectivity, repeatability, reproducibility, robustness, etc. of application in analytical chemistry. As in chemical analysis, the process of sampling, ensuring the integrity, representativity and traceability of the sample, is of capital importance in the dating analytical process.

Calibration (involving the disposal of a set of samples of known age) and analysis of errors are of crucial importance for dating. In general, there is no possibility of constructing a universal calibration curve for a given method and time-dependent local and regional factors have to be considered. Available methods of dating cover a wide range of time intervals but depending on the age of the geological or archeological object under study, different methods have to be used. Importantly, in the most cases consistent dating from two or more independent methods is accessible. Overall, dating can be viewed as an active research field where new developments are enhancing the scope of suitable methodologies.

General literature

Aitken MJ (1990) Science-based dating in archaeology. Longman, New York.
Bowen R (1994) Isotopes in the Earth sciences. Chapman & Hall, London.
Bowen R, Attendorn H-G (1997) Radioactive and stable isotope geology. Chapman & Hall, London.
Bowen R (2011) Radioactive dating methods. In: Vertés A, Nagy S, Klencsár Z, Lovas RG, Rösch F (eds) Handbook of nuclear physics, 2nd edn. Springer, Heidelberg, chapter 17.
Butler RF (1992) Paleomagnetism. Magnetic domains to geologic terranes. Blackwell, Boston.
Dunai T (2010) Cosmogenic nuclides. Cambridge Univ. Press, Cambridge.
Geyh MA, Schleicher H (1990) Absolute age determination—physical and chemical dating methods and their application. Springer, Berlin-Heidelberg.
Gillespie R (1984) Radiocarbon user's handbook, Oxford University Committee for Archaeology. Oxbow Books, Oxford.
Ikeya M (1993) New applications of electron spin resonance—dating, dosimetry and microscopy. World Scientific, Singapore.
Lahiri S, Maiti M (2011) Methods of cosmochemical analysis. In: Vertés A, Nagy S, Klencsár Z, Lovas RG, Rösch F (eds) Handbook of nuclear physics, 2nd edn. Springer, Heidelberg, chapter 54.
Renfrew C, Bahn P (1991) Archaeology: theory, methods and practice. Thames & Hudson, London, chapter 4.

Acknowledgments The author wish to thank Prof. Fritz Scholz for helpful discussion during the preparation of the manuscript. Financial support is gratefully acknowledged from the MICIN Projects CTQ2011-28079-CO3-02 and CTQ2014-53736-C3-2-P.

Appendix 1: Analysis of errors and calibration

In the most simple case, dating is performed by measuring a time-dependent quantity, $y(t)$, of the sample under study providing that the value of that quantity of a reference system at time-zero, $y(0)$, and its dependence, i.e., the rate of variation of this quantity with time, are known.

In several cases, the variation of $y(t)$ with time can be fitted to a mathematical function. This is the case for the amount of chemical alteration products, which, in the case of metal corrosion, follows a potential law:

$$y(t) = at^{b} \tag{27}$$

In the obsidian method (vide infra), it is accepted that $b = 1/2$. To estimate the accuracy of the age determination, it is necessary to take into account different sources of errors, including those called systematic and those called accidental. First of all, there are systematic errors resulting from biased laboratory operations, sample contamination and/or biased calibrations.

Apart from the above errors, there are 'accidental' or random errors appearing as a result of non-controllable fluctuations in the measurement process determining the precision of the measurement series. Those errors are usually described in terms of a Gaussian function of error and are minimized by performing replicate measurements (because the random error is proportional to the inverse of the square root of the number of replicate measurements). Then, the representative value of the measured quantity is the arithmetic average of the measured values and its error is typically expressed in terms of the standard deviation, σ, whose meaning is that there is a 68 % probability that the 'true' value of the measured quantity, y, lies within the range $y \pm \sigma$. A frequent, more restrictive, criterion is to express the measurements as $y \pm 3\sigma$; this range corresponds to a probability of 99.7 % comprising the 'true' value of the measured quantity.

The uncertainty in the measured age, Δt, can be evaluated using the conventional theory of error propagation so that:

$$\frac{\Delta t}{t} = \frac{1}{a}\left(\frac{\Delta y}{y}\right) + \left(\frac{\Delta a}{a}\right) + \ln t \left(\frac{\Delta b}{b}\right) \quad (28)$$

In the above equation, $\left(\frac{\Delta a}{a}\right)$ and $\left(\frac{\Delta b}{b}\right)$ represent the relative uncertainty in the parameters a and b, which should be estimated from calibration data, and can in principle be taken as time independent. The term $\left(\frac{\Delta y}{y}\right)$ denotes the relative uncertainty of the measured quantity. The above equation predicts that, even if these two last relative uncertainties remain constant (a situation that applies in several instrumental methods), the uncertainty in the age increases with the age of the sample. In most cases, however, it is more realistic to assume that the 'absolute' uncertainty in the measured quantity remains constant (its lower value would be given by the lowest division of the scale of the instrument used for measurements). Then, Eq. (28) can be rewritten as:

$$\frac{\Delta t}{t} = t^{-b}\left(\frac{\Delta y}{ab}\right) + \left(\frac{\Delta a}{a}\right) + \ln t \left(\frac{\Delta b}{b}\right) \quad (29)$$

Figure 18 illustrates the time variation of the different terms of $\left(\frac{\Delta t}{t}\right)$ and the sum of the same using arbitrary values for the case $b = 1/2$ One can see that the uncertainty varies on the age as depicted in Fig. 19. This implies that, for improving the precision in the age measurement of 'old' samples, it is necessary to minimize the error contributions of the calibration and the measurements of the age-dependent quantity. This could involve special instrumental requirements, as is the case for radiocarbon dating using the counting methodology, as detailed in the corresponding section.

In general, calibration using a set of samples of known age is required for accurate age determination. In the most favorable case, a 'universal' calibration curve, given by a monotonically increasing or decreasing variation of the time-dependent property $y(t)$ with time valid for all sites in the Earth, could be constructed. In practice, however, there are a variety of factors influencing the values of $y(t)$ so that there is no possibility of constructing a universal calibration curve for dating using a given method. The case of radiocarbon dating is particularly illustrative: the calibration curve separates from the theoretical expected for radioactive decay as a result, among others, of the extensive combustion of carbon and petroleum derivatives in the last two centuries. Additionally, 'local' variations (for instance, latitude effects) can appear so that not only the composition of the sample under study but also of its environment can be of crucial importance. In fact, in buried samples, the depth of the burial can be a decisive factor conditioning the application of several dating methods. In general, therefore, 'local' or 'regional' calibration curves have to be used for dating purposes. Of course, reproducibility of the results is an essential property which has to be ensured via inter-laboratory trials.

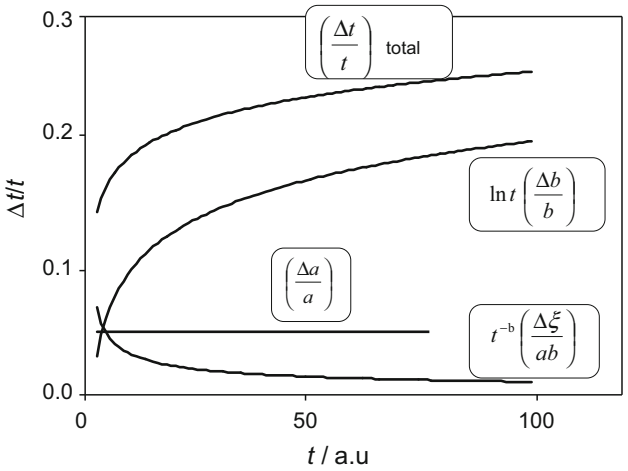

Fig. 18 Time variation of the relative uncertainty in age determination for a method based on a potential law of aging using Eq. (29) for the case $b = 1/2$

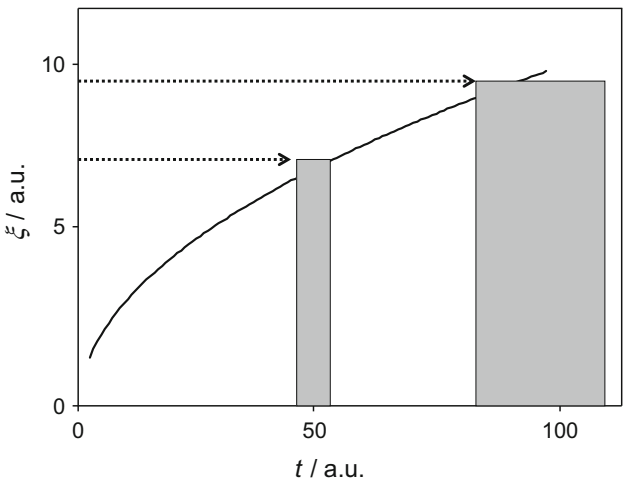

Fig. 19 Interval of error at two different ages using the potential law of aging described by Eq. (29) for the case $b = 1/2$

Appendix 2: Growth marks methods

Although, strictly, methods of dating based on the examination of grow marks do not fall within the category of physical and chemical methods of dating, it may be instructive to provide a short overview of the same. Their inclusion here obeys not only to their (in principle) conceptual simplicity, but also to their historical significance as precursors, to some extent, of physical and chemical dating methods as well as by the fact that they have been (and are) used as 'reference methods' for instance, for radiocarbon calibration.

Dendrochronology or tree-ring dating was invented in the early decades of the twentieth century by astronomer A. E. Douglass and archeologist C. Wissler [1]. The method is based on the fact that, in temperate regions (and in some tropical zones), trees build up one visible ring per calendrical year so that the counting of the rings provides the time of life of the tree. Visible rings result from the change in growth rate through the seasons of the year. In the early period of the growing season, growth is relatively fast and the inner region of the growth ring is formed. This region ('early wood' or 'spring wood') is less dense than the outer region, where the growth rate is lowered ('late wood' or 'summer wood').

The thickness and structure of the rings reflect the climatic and environmental conditions in which the tree grew so that a characteristic ring pattern is recorded. This pattern forms a characteristic signature of narrow and broad rings which permits to define specific signature for periods of years. Ring series contain historical and ecological information that is related to competition, release, fire, climate, insect attacks, etc. This pattern can be compared and matched ring for ring with trees growing in the same geographical zone and under similar climatic conditions resulting in cross-dating which leads to the determination of the age of a given wood sample [2]. To eliminate individual variations in tree-ring growth, the smoothed average of the tree-ring widths of multiple tree samples is taken, thus defining a 'ring history', a process termed as replication. A tree-ring history whose beginning and end dates are not known is called a floating chronology. It can be anchored by cross-matching a section against another chronology (tree-ring history) whose dates are known.

Using this procedure, absolute dating is made possible. Fully anchored chronologies have been obtained for river oak trees from South Germany, pine wood from Northern Ireland and bristlecone pine wood from California [3]. Furthermore, the mutual consistency of these independent dendrochronological sequences has been confirmed by comparing their radiocarbon and dendrochronological ages. Currently, the tree-ring data series has been extended to 13,900 years and used to calibrate radiocarbon dating [4].

A similar methodology can be used for dating purposes on the basis of different stratified growing systems. A pictorial representation for correlating the age of different specimens is depicted in Fig. 20.

Correlation between layers of the same age is a well-known methodology for relative dating in geology typically aided by petrographic analysis and fossil markers. There is a variety of dating methods based on the account of growth lines associated with daily, seasonal or annual periods on geological features and living organisms. Seasonal patterns occur in ice cores, layered deposits (varves) in a glacial, lake, river or sea bed [5], but also in the otoliths of fish [6] and in the spines of columnar cactus (acanthochronology) [7]. These methods are used in combination with radiocarbon, isotope enrichment and other methods for dating. The chronology of clusters of lakes with varved sediments in central North America, Canadian Arctic, and in northern and central Europe, based on varved records (typically 200–500 cm long) covering a period of 1,000–2,000 years has been recently reviewed [5]. A particularly interesting approach was derived from the study of growth bands in corals and shells. This will be treated in the Appendix 3 in relation with the age of the Earth.

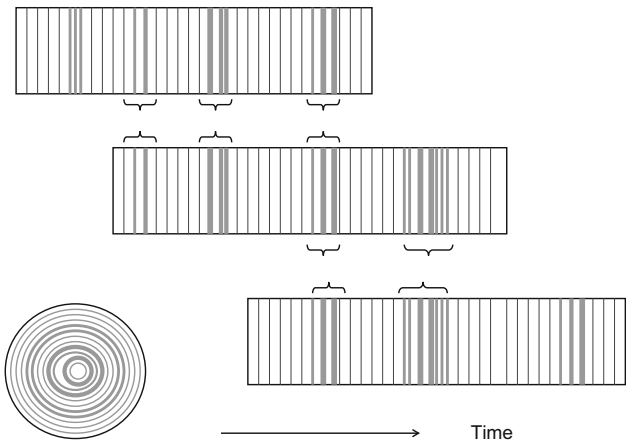

Fig. 20 Scheme for the correlation of different tree rings. Signature periods of years are connected

References

[1] Douglass AE (1909) Weather cycles in the growth of big trees. Monthly Weather Review 37:225−237.

[2] McGovern PJ, Sever TL, Myers JW, Myers EE, Bevan B, Miller NF, Bottema S, Hongo H, Meadow RH, Kuniholm PI, Bowman SGE, Leese MN, Hedges REM, Matson FR, Freestone IC, Vaughan SJ, Henderson J, Vandiver PB, Tumosa CS, Beck CW, Smith P, Child AM, Pollard AM, Thuesen I, Sease C (1995) Dendrochronology science in archaeology: a review. Am J Arcaheol 99:79–142.

[3] Minze S, Kromer B, Becker B, Ferguson CW (1986) Radicarbon age calibration back to 13,300 years BP and the 14C age matching of the German Oak and US Bristlecone Pine chronologies. Radiocarbon 28:969–979.

[4] Reimer PJ, Bard E, Bayliss A, Beck JW, Blackwell PG, Ramsey CB, Buck CE, Cheng H, Edwards RL, Friedrich M, Grootes PM, Guilderson TP, Aflidason H, Hajdas I, Hatté C, Heaton TJ, Hoffmann DL, Hogg AG, Hughen KA, Kaiser KF, Kromer B,

Manning SW, Niu M, Reimer RW, Richards DA, Scott EM, Southon JR, Staff RA, Turney CSM, van der Plicht J (2013) IntCal 113 and Marine 13 radiocarbon age calibration curves 0–50,000 years - cal BP. Radiocarbon 55:1869–1887.

[5] Ojala AEK, Francus P, Zolistchka B, Besonen M, Lamoureux SF (2012) Characteristics of sedimentary varve chronologies—a review. Quater Sci Rev 43:45–60.

[6] Campana SE (2001) Accuracy, precision and quality control in age determination, including a review of the use and abuse of age validation methods. J Fish Biol 59:197–242.

[7] English NB, Dettman DL, Sandquist DR, Williams DG (2010) Daily to decadal patterns of precipitation, humidity, and photosynthetic physiology recorded in the spines of the columnar cactus, *Carnegiea gigantea*. J Geophys Res 115:G02013.

Appendix 3: The age of the Earth and the sun

Determining the age of the Earth and the sun has claimed considerable attention historically. For instance, Newton presented in the *Principia,* a thought experiment to show that a large body like the Earth made of molten iron would take about 50,000 years to cool. He first estimated the time it would take to cool for a "globe of iron of an inch in diameter, exposed red hot to open air". Buffon's experiments concluded that if the Earth had been made of molten iron, the Earth would require 42,964 years to cool below incandescence and 96,670 years to cool to the present temperature [1].

William Thomson (Lord Kelvin) reported between 1863 and 1897 a series of estimates of the age of the Earth based on experiments on molten sphere at 2,000 °C, and determined the amount of time it would take for the near surface to cool to its present temperature [2, 3]. The surface of such a molten globe will cool very rapidly while the interior remains hot, so that after a time t, the surface temperature will reach the contemporary value (averaged to 0 °C). Present-day measurements give an average value of about 6.7×10^{-2} w/m^2 for the irradiated energy per surface unit which is smaller than the total solar flux incident on the Earth, 1.4×10^3 w/m^2. Although the 'internal' flux is negligible in the surface energy balance, its knowledge could be used to estimate the Earth's age as noted by several authors before Kelvin, including Fourier and Buffon. Kelvin, based on estimates of the thermal diffusivity of rocks, calculated for the Earth's initial temperature a value of 3,900 °C [4–6]. The Kelvin calculations, logically ignoring the heat produced by radioactive decay and the head released via convection in the mantle, gave values of the age of the Earth between 20 and 40 million years old. The convection contribution can be considered as particularly significant, as suggested in 1895 by Perry [6–8]. Calculations using Perry's model along with modem estimates for the thermal diffusivity and freezing point of mantle rock provide Earth's ages as great as 2 billion or 3 billion years [9].

These values were consistent with the calculations on the age of the sun performed independently by Helmholtz (1856) [10] and Newcomb (1892) based on a model of sun formation via condensation from a nebula of gas and dust. Helmholtz proposed his model of solar formation via gravitational collapse after discarding the possibility of a chemical origin (using known combustion heats) of the solar energy [11, 12]. Kelvin considered an alternative model for explaining the solar radiation resulting from the continuous bombardment of meteorites. Kelvin rejected this model in 1861 because there was no observational evidence of such meteorite bombardment and the effect of the additional mass of the sun on the period of rotation of the Earth—by reasons of angular momentum conservation—would have been detected. Accordingly, Kelvin finally accepted the Helmholtz's theory of gravitational contraction [4].

The above, essentially 'physical', methods for calculating the age of the Earth and the sun were often in conflict with 'geological' approaches to the same problem. Since the seminal discovery of Steno in the seventeenth century and Smith in the 18th one of the connection between fossils and sedimentary strata, the geologists supported in general the idea that periods of time of several millions of years were necessary for creating the Earth's crust [13]. In 1860, Phillips utilized sediment accumulation to estimate the Earth's age at 38–96 million years whereas Walcott obtained values between 30 and 80 million years based on erosion/sedimentation calculations.

Another source of geological approximations was derived from salinity of oceans. Halley first considered this possibility upon arguing that rivers are continually washing small amounts of dissolved salts into the oceans, so that accounts of salinity could provide an estimate of the time taken for an initially fresh water ocean to achieve its current level of salinity. Using sodium concentrations as a marker, Joly calculated in 1899 an oceanic age between 90 and 100 million years.

In 1864, Croll proposed a hypothesis linking the onset of the ice ages to changes in the eccentricity of the Earth's orbit, further suggesting that the calculated dates of periods of high orbital eccentricity might be used to determine the date of the most recent glacial period [14–16]. Lyell combined this approach with statistical data on fossils (series of tertiary molluscs) concluding that a complete

replacement of species (revolution) would require 20 million years. Assuming that this time was the same in all geological times, the twelve revolutions that he estimated had occurred since the Cambrian, leading to an Earth's age (sedimentary Earth's age) of 240 million years [17].

Astronomical methods of dating were also proposed for solving the problem of the age of the sun and the planets. Kelvin estimated the Earth's age from tidal effects. In short, the tides rise and fall causes a frictional effect on the marine bed resulting in a reduction in the Earth's rotation, an effect earlier discussed by G. H. Darwin [18–20]. By reasons of conservation of angular momentum, the orbital velocity of the Moon increases and this increase yields an increase in the Moon's distance from Earth. Calculations from tidal effects elevated the age of the Earth to 10^9 years. Another astronomical method, based on the change of the eccentricity of Mercury's orbit over time, was reported by Harold Jeffreys in 1918, produced an age of 3×10^9 years for the solar system [21].

In certain modern corals and shellfish, we find growth bands that indicate yearly, monthly, and even daily growth, rather like the annual rings that trees produce. Similar to tree ring counting, the number of growth bands of a specimen of coral or shellfish is indicative of its lifetime. We can also see that there are about thirty daily bands per month and about 365 daily bands per year for modern corals and shellfish. In contrast, Wells recorded a number of growth bands in Devonian corals larger than in contemporary corals [22, 23]. Subsequent paleontological data suggested that there was an almost uniform increase in the number of days per year during geological times when the usual U-based chronology is used [24]. The increase in the number of days of the year since the Devonian would be the result of the lowering of the terrestrial rotation rate due to the friction associated with tides. This is an interesting example of circularity/complementarity in dating procedures. If a method for estimating the rate of variation of tidal effects with geological time was available, the age of the strata could be calculated from the count of annual growth lines of corals. Then, a coral-based geological time scale could be constructed and then compared to the U-based scale [24]. The currently accepted age of the Earth is of 4.54×10^9 years, based on radiometric uranium dating of meteorites judged to be of the time of the formation of our planet, combined with concomitant data for lunar and terrestrial samples considered as the oldest using geological criteria [25].

Currently, the age of the Earth is estimated as long as 4.54 ± 0.05 billion years. This age is based on calculations from radiometric dating of calcium–aluminum-rich inclusions in meteorites and is consistent with the ages of the oldest known terrestrial materials (zircons from Jack Hills formation in Australia) and lunar samples. It is assumed that the Sun condensed in the central part of a primordial nebula in rotation. The gravitational contraction finally resulted in the formation of a central proto-star surrounded by a proto-planetary disk subsequently forming planets by accretion. The above age of the Earth would be that estimated for the beginning of the accretion of materials originating the planets and meteorites [26].

References

[1] Burchfield JD (1998) The age of the Earth and the invention of geological time. Geological Society, London, Special Publications 143:137–143.
[2] Kelvin WT (1863) On the secular cooling of the Earth. Trans Roy Soc Edinburgh 23:157−170.
[3] Kelvin WT (1895) On the age of the Earth. Nature 51:438−440.
[4] Burchfield JD (1990) Lord Kelvin and the age of the Earth. Univ. Chicago Press, Chicago.
[5] Dalrymple GB (1994) The age of the Earth. Stanford Univ. Press, Stanford.
[6] Perry J (1895) On the age of the Earth. Nature 224−227.
[7] Perry J (1895) On the age of the Earth. Nature 341−342.
[8] Perry J (1895) On the age of the Earth. Nature 582−585.
[9] England PC, Molnar P, Richter FM (2007) Kelvin, Perry and the age of the Earth. American Scientist 95:342−349.
[10] von Helmholtz H (1856) On the interaction of natural forces. Phil Mag 11:489–578.
[11] Stinner A (2002) Calculating the age of the Earth and the Sun. Phys Educ 37:296–305.
[12] Tort AC, Nogarol F (2011) Another look at Helmholtz's model for the gravitational contraction of the Sun. Eur J Phys 32:1679−1685.
[13] Brookfield ME (2004) Principles of Stratigraphy. Blackwell, London.
[14] Croll J (1864) On the physical cause of the change of climate during geological epochs. Philos Mag ser. 4, 28:121−137.
[15] Croll J (1867) On the eccentricity of the Earth's orbit and its physical relations to the glacial epoch. Phil Mag ser. 4, 33:119−131.
[16] Croll J (1868) On geological time, and the probable date of the glacial and upper Miocene period. Phil Mag ser. 4, 35:363−384 & 36:141−154, 362−386.
[17] Lyell C (1867) Principles of geology 10th edition, Murray, London, Darwin, G.H.
[18] Darwin GH (1877) On the influence of geological changes on the Earth's axis of rotation. Phil Trans Roy Soc London 167:271.

[19] Darwin GH (1879) On the precession of a viscous spheroid and on the remote history of the Earth. Phil Trans Roy Soc London 170, 447−530.
[20] Darwin GH (1880) On the secular change of the orbit of a satellite revolving about a tidally distorted planet. Phil Trans Roy Soc London 171, 713−891.
[21] Jeffreys H (1924) The Earth. Cambridge Univ. Presss, Cambridge.
[22] Wells JW (1963) Coral growth and geochronometry. Nature 167:948−950.
[23] Raup DM, Stanley SM (1971) Principles of paleontology. Freeman & Co. San Francisco.
[24] Scrutton CT (1978) Periodic growth features in fossil organisms and the length of the day and month in tidal friction and the Earth's rotation. Springer, Berlin, pp 154−196.
[25] Dalrymple GB (2001). The age of the Earth in the twentieth century: a problem (mostly) solved. Special Publications, Geological Society of London 190:205–221.
[26] Audouze J, Israël G, Eds (1985) The Cambridge atlas of astronomy. Cambridge Univ Pres, Cambridge.

Appendix 4: The Shroud of Turin and radiocarbon dating

The Shroud of Turin is a piece of linen cloth, conserved in the Cathedral of Saint John the Baptist in Turin, Italy, whose origin and its impressed image are the subject of intense debate among theologians and historians. As it is well known, the cloth exhibits the image of a man who appears to have suffered diverse traumatisms consistent with crucifixion. The negative image, first observed in 1898 on the photographic plate obtained by Secondo Pia, offered this image much more clearly than the natural sepia color of the shroud (see Figs. 21, 22).

In 1978, a multidisciplinary research conducted through The Shroud of Turin Research Project (STURP) found no reliable evidence of how the image was produced. In 1988, a series of radiocarbon dating tests were performed in the laboratories of the universities of Oxford and Arizona and the Swiss Federal Institute of Technology, dating the tested samples between 1,260 and 1,390, i.e., in the Middle Age, using the accelerator mass spectrometry technique [1]. On the morning of 21 April 1988, four samples, of ca. 50 mg each, were excised by G. Riggi in the presence of Cardinal Anastasio Ballestrero (Archbishop of Turin), the scientific advisers Professors Gonella (Turin Polytechnic) and Tite (British Museum), two textile experts (Professors Testore and Vial), accompanied by Professors Damon, Donahue, Hall, Hedges and Woelfli, representatives of the three radiocarbon-dating laboratories [1]. As control samples, two linen samples from a tomb excavated at Qasr Ibrîm in Nubia and the mummy of Cleopatra from Thebes and threads removed from the cope of St Louis d'Anjou were used [1].

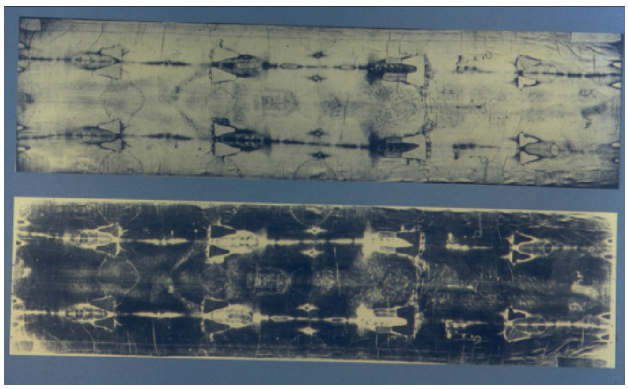

Fig. 21 The Turin Shroud. *Top* normal view; *bottom* negative view. Photograph Alberto Pizzoli/Corbis, with permission

Fig. 22 The head visible on the Shroud (normal view). Photograph Alberto Pizzoli/Corbis, with permission

Each laboratory fractioned the samples and performed different pretreatments on them. All the groups combusted the cleaned textile subsample with copper oxide in sealed tubes, then converted the resulting CO_2 to graphite targets. Because the shroud had been exposed to a wide range of potential sources of contamination and because of the uniqueness of the samples available, blind-test procedures were not performed. The conventional radiocarbon ages were all calculated using the procedures suggested by

Table 5 Dating of samples from the Shroud of Turin from Refs. [1, 3]

Sample	Mean date (year BP)	Calendar date ranges
1	691 ± 31	AD 1,273–1,288
2	937 ± 16	AD 1,032–1,048, 1,089–1,119, 1,142–1,154 cal
3	1,964 ± 20	AD 11–64 cal
4	724 ± 20	AD 1,268–1,278 cal

Confidence limits on the radiocarbon scale found from the standard error on the unweighted mean, assuming a t_5 distribution (multiplying factor of 1.1 for 68 % confidence level). Standard error estimated from scatter

Stuiver and Polach [2], with normalization to $\delta^{13}C = -25$ ‰, and were accordingly reported in yr BP (years before 1950). Table 5 shows the data for calibrated date ranges at the 68 % confidence level [1].

During the last decades, a variety of analysis, including fibers composition, pollen content, anatomical studies, image and text analysis, has been performed frequently with contradictory results regarding the age and image formation. This last has been the subject of different hypotheses: from irradiation by ultraviolet, X-ray, etc. to chemical processes such as the Maillard reaction.

The radiocarbon dating has been questioned with regard to the choice of the sample taken for testing. In this view, the samples for radiocarbon dating could correspond to a medieval textile repair fragment rather than the original cloth. According to Rogers [3], chemical tests suggested the presence of vanillin in the radiocarbon sample and in the Holland cloth, but not the rest of the shroud. The levels of vanillin, which is produced by the thermal decomposition of lignin, a chemical compound found in plant material such as flax, should decrease over time, leading to age estimates between 1,300 and 3,000 years old.

Although it has been proposed that radiocarbon dating could be distorted due to neutron irradiation from an unknown source, no evidences supporting this possibility can be adduced [4]. The most recent contribution in this line hypothesizes that high-frequency pressure waves generated in the Earth's crust during an Earthquake could have produced significant neutron emissions. Such emissions could have interacted with nitrogen atoms in the linen fibers, inducing chemical reactions that created the distinctive face image on the shroud and also could have lead to a modification in the radiocarbon signature [5]. Such approaches, however, must be viewed with extreme caution due to their highly speculative character.

References

[1] Damon PE, Donahue DJ, Gore BH, Hatheway AL, Jull AJT, Inc. TW, Sercel PJ, Toolin LJ, Bronk CR, Hall ET, Hedges REM, Housley R, Law IA, Perry C, Bonani G, Trumbore S, Woelfli W, Ambers JC, Bowman SGE, Leese MN, Tite MS (1989) Radiocarbon dating of the Shroud of Turin. Nature 337:611−615.

[2] Stuiver M, Polach H (1977) Discussion: reporting of ^{14}C data. Radiocarbon 19:355-363.

[3] Rogers RN (2005) Studies on the radiocarbon sample from the Shroud of Turin. Thermochim Acta. 425:189–194.

[4] Phillips TJ (1989) Shroud irradiated with neutrons? Nature 337:594 (the reply of Edges REM in Nature 337:594).

[5] Carpinteri A, Lacidogna G, Borla O (2014) Is the Shroud of Turin in relation to the Old Jerusalem historical Earthquake? Meccanica. doi:10.1007/s11012-013-9865-x.

Appendix 5: The KBS tuff controversy

A paradigmatic example of the importance and difficulty in dating was the so-called KBS tuff controversy. The KBS tuff (for "Kay Behrensmeyer Site", after the geologist who first described it) is a layer of redeposited volcanic ash which lies in the Koobi Fora geological formation (Pleistocene) in East Turkana region of Kenya where the expeditions leaded by Leakey collected an important set of hominid fossils between 1968 and 1973 [1]. The most relevant aspect would be the appearance of fossils attributable to the genus *Homo* (the famous KNM-ER 1,470 specimen, see Fig. 23), a skull with relatively large cerebral cavity, at strata of an apparent age of 2.6 million years, therefore, contemporary of *Australophitecus*. This discovery implied an important revision of our paleontological history, because the dominant view considered that *Homo* appeared at least 1 million years later, thus obliging to a revision of the man's evolutionary scheme [2].

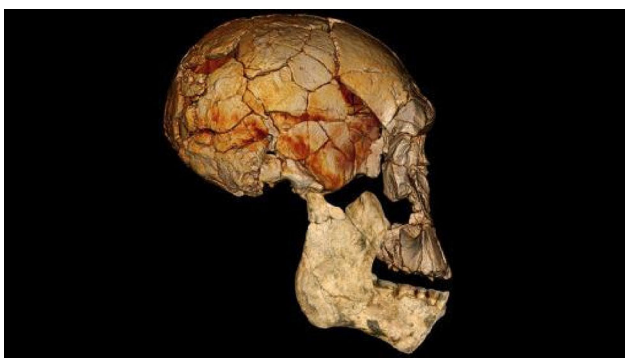

Fig. 23 Image of the The KNM-ER 1470 specimen after its reconstruction. Courtesy of F. Spoor, Max Planck Institute, with permission

Dating the so-called KBS tuff was considered crucial. Using the $^{39}Ar/^{40}Ar$ method, Fitch and Miller dated initially feldspar from the tuff as long as 2.61 ± 0.26 million years [3]. However, Curtis et al., using the conventional potassium–argon technique, reported values of 1.60 and 1.82 million years from KBS tuff samples of the Koobi Fora formation [4], essentially in agreement with paleontological data from Cooke [5]. Dating of zircons from the KBS tuff using the fission-track method Hurford et al. [6] obtained an age of 2.44 ± 0.08 million years, revised by Fitch et al. to 2.42 million years [7, 8]. Further studies, however, confirmed the 'youngness' of the KBS tuff, for which the most recent dating are of 2.058 ± 0.034 million years [9] and 2.03 ± 0.05 million years [10].

References

[1] Isaac GL, Leakey REF, Behrensmeyer AK (1971) Archeological traces of early hominid activities, East of Lake Rudolf, Kenya. Science 173:1129−1134.

[2] Lewin R (1987) Bones of contention. Controversies in the search of human origins. Simon & Schuster, New York.

[3] Fitch FJ, Miller JA (1970) Radioisotopic age determinations of Lake Rudolf artefact site. Nature 226:226−228.

[4] Curtis GH, Drake RE, Cerling TE, Cerling BW, Hampel JH (1975) Age of KBS Tuff in Koobi Fora Formation, East Rudolph, Kenya. Nature 258:395−398.

[5] Cooke HBS (1978) Suid evolution and correlation of African hominid localities: an alternative taxonomy. Science 201:460−463.

[6] Hurford AJ, Gleadow AJW, Naeser CW (1976) Fission-track dating of pumice from the KBS Tuff, East Rudolf, Kenya. Nature 263:738−740.

[7] Fitch FJ, Hooker PJ, Miller JA (1976) $^{40}Ar/^{39}Ar$ dating of the KBS Tuff in Koobi Fora Formation, East Rudolf, Kenya. Nature 263:740−744.

[8] Hay RL (1980) The KBS tuff controversy may be ended. Nature 284:401−403.

[9] Joordens JCA, Dupont-Nivet G, Feibel CS, Spoor F, Sier MJ, van der Lubbe JHJL, Nielsen TK, Knul MV, Davies GR, Vonhof HB (2013) Improved age control on early Homo fossils from the upper Burgi Member at Koobi Fora, Kenya. J Hum Evol 65:731−745.

[10] McDougall I, Brown FH, Vasconcelos PM, Cohen BE, Thiede DS, Buchanan MJ (2012) New single crystal 40Ar/39Ar ages improve time scale for deposition of the Omo Group, Omo-Turkana Basin, East Africa. J Geol Soc 169:213–226.

References

1. Burchfield JD (1998) The age of the Earth and the invention of geological time. Geol Soc Lond Spec Publ 143:137–143
2. McCarthy DD (1991) Astronomical time. Proc IEEE 79:915–920
3. Newton I (1687) Philosophiae Naturalis Principa Mathematica. Londini, Jussu Societatis Regiae ac Typis J. Streater, or The Mathematical Principles of Natural Philosophy, English translation by Motte A. London, 1700s
4. Landau LD, Lifshitz EM (1976) Mechanics in course of theoretical physics, vol 1. Butterworth-Heinemann, London
5. Landau LD, Lifshitz EM (1977) Quantum mechanics in course of theoretical physics, vol 3. Butterworth-Heinemann, London
6. For the philosophical aspects of analytical chemistry and ultimately the so-called analytical paradigm, see Malissa H (1989) Philosophical aspects of analytical chemistry. Fresenius Z Anal Chem 333:285–292
7. Wagner G (1995) Altesbestimmung von jungen Gesteinen und Artefakten. Enke Verlag, Stuttgart
8. Aitken MJ (1990) Science-based dating in archaeology, chapter 1. Longman, New York
9. Yavorski BM, Detlaf AA (1977) Handbook of physics. Mir, Moscow, pp 907–911
10. Libby WF (1946) Atmospheric helium three and radiocarbon from cosmic radiation. Phys Rev 69:671–672
11. Anderson EC, Libby WF, Weinhouse S, Reid AF, Kirshenbaum AD, Grosse AV (1947) Radiocarbon from cosmic radiation. Science 105:576–577
12. Arnold JR, Libby WF (1949) Age determinations by radiocarbon content: checks with samples of known age. Science 110:678–680
13. Scholz G, Scholz F (2014) First-order differential equations in chemistry. ChemTexts 1:1
14. McNichol AP, Jull ATS, Burr GS (2001) Converting AMS data to radiocarbon values: considerations and conventions. Radiocarbon 43:313–320
15. Bowman S (1995) Radiocarbon dating. British Museum Press, London
16. Ferronsky VI, Polyakov VA (2012) Isotopes of the Earth's hydrosphere. Springer, New York
17. Stuiver M, Long A, Kra RS (eds) (1993) Calibration. Radiocarbon 35:1–244
18. de Vries H (1958) Variations in concentration of radiocarbon with time and location on Earth. In: Proceedings, Ned Akad Wetenschappen, Series B61:l
19. Suess HE (1970) Bristlecone-pine calibration of radiocarbon time 5200 B.C. to present. In: Olsson IU (ed) Radiocarbon variations and absolute chronology. Almqvist and Wiksell, Stockholm, pp 303–312
20. Stuiver M, Polach HA (1977) Discussion: reporting of ^{14}C data. Radiocarbon 19:355–363
21. Stuiver M, Reimer PJ, Braziunas TF (1998) High-precision radiocarbon age calibration for terrestrial and marine samples. Radiocarbon 40:1127–1151
22. Reimer PJ, Baillie MGL, Bard E, Bayliss A, Beck JW, Bertrand CJH, Blackwell PG, Buck CE, Burr GS, Cutler KB, Damon PE, Edwards RL, Fairbanks RG, Friedrich M, Guilderson TP, Hogg AG, Hughen K, Kromer B, McCormac G, Manning S, Ramsey CB, Reimer RW, Remmele S, Southon JR, Stuiver M, Talamo S, Taylor FW, van der Plicht J, Weyhenmeyer CE (2004) INTCAL04 terrestrial radiocarbon age calibration, 0–26 cal kyr BP. Radiocarbon 46:1029–1058
23. The most recent revision can be seen in Reimer PJ, Bard E, Bayliss A, Beck JW, Blackwell PG, Ramsey CB, Buck CE, Cheng H, Edwards RL, Friedrich M, Grootes PM, Guilderson TP,

Aflidason H, Hajdas I, Hatté C, Heaton TJ, Hoffmann DL, Hogg AG, Hughen KA, Kaiser KF, Kromer B, Manning SW, Niu M, Reimer RW, Richards DA, Scott EM, Southon JR, Staff RA, Turney CSM, van der Plicht J (2013) IntCal 113 and Marine 13 radiocarbon age calibration curves 0–50,000 years cal BP. Radiocarbon 55:1869–1887
24. Davis R, Schaffer OA (1955) Chlorine-36 in nature. Ann N Y Acad Sci 62:105–122
25. Fröhlich K, Lübert J (1973) Uber die Möglichkeit der Messung von Erosionsgeshwindigkeiten an oberflächengesteinen mit den natürlichen Radionuckliden ^{41}Ca und ^{39}Ar. Z Angew Geol 19:550
26. Cockburn HAP, Summerfield MA (2004) Geomorphological applications of cosmogenic isotope analysis. Progr Phys Geogr 28:1–42
27. Ferronsky VY, Polyakov VA (2012) Origin and production of cosmogenic radioisotopes in Isotopes of the Earths hydrosphere. Springer, Berlin, pp 215–228
28. Falkowski P, Scholes RJ, Boyle E, Canadell J, Canfield D, Elser J, Gruber N, Hibbard K, Högberg P, Linder S, MacKenzie FT, Moore B, Pedersen T, Rosenthal Y, Seitzinger S, Smetacek V, Steffen W (2000) The global carbon cycle: a test of our knowledge of Earth as a system. Science 290:291–296
29. Granger D (2006) A review of burial dating methods using ^{26}Al and ^{10}Be. In: Siame L, Bourlès D, Brown E (eds) In-situ-produced cosmogenic nuclides and quantification of geological processes. Geological Society of America Special Paper, vol 415. Geological Society of America, pp 1–16
30. Balco G, Shuster DL (2009) ^{26}Al–^{10}Be–^{21}Ne burial dating. Earth Planet Sci Lett 286:570–575
31. Farley KA, Libarkin J, Mukhopadhyay S, Amidon W (2006) Cosmogenic and nucleogenic ^{3}He in apatite, titanite, and circon. Earth Planet Sci Lett 248:451–461
32. Niedermann S (2002) Cosmic-ray-produced noble gases in terrestrial rocks: dating tools for surface processes, noble gases in geochemistry and cosmochemistry. Rev Miner Geochem 47:731–784
33. Eugster O, Herzog GF, Marti K, Caffee MW (2006) Irradiation records, cosmic-ray exposure ages, and transfer times of meteorites in meteorites and the early solar system II. In: Lauretta DS, McSween HY (eds) University of Arizona Press, Tucson, pp 829–851
34. Audouze J, Israël G (eds) (1985) The Cambridge atlas of astronomy. Cambridge University Press, Cambridge, p 57
35. Urey HC (1948) Oxygen isotopes in nature and in the laboratory. Science 108:489–496
36. Emiliani C (1955) Pleistocene temperatures. J Geol 63:538–578
37. Smits F, Gentner W (1950) Argonbestimmummungen an Kalium-Mineralien I. Bestimmungen an tertiären Kalisalzen. Geochim Cosmochim Acta 1:22–27
38. Hodson MH (1973) Closure temperature in cooling geochronological and petrological systems. Contr Miner Pet 40:259–274
39. Merrihue CM (1965) Trace-element determinations and potassium–argon dating by mass spectroscopy of neutron irradiated samples. EOS Trans Am Geophys Union 46:125 (abstr)
40. Merrihue CM, Turner G (1966) Potassium–argon dating by activation with fast neutrons. J Geophys Res 71:2852–2857
41. Yavorski BM, Detlaf AA (1977) Handbook of physics. Mir, Moscow, p 858
42. Yavorski BM, Detlaf AA (1977) Handbook of physics. Mir, Moscow, p 865
43. Geyh MA, Schleicher H (1990) Absolute age determination—physical and chemical dating methods and their application. Springer, Berlin, Heidelberg, pp 261–263
44. Wagner GA, Van den haute P (1992) Fission track-dating. Kluwer, Dordrecht
45. Van den haute P, De Corte F (1998) Advances in fission-track geochronology. Kluwer, Dordrecht
46. Li W, Wang L, Lang M, Trautmann C, Ewing RC (2011) Thermal annealing mechanisms of latent fission tracks: apatite vs. zircon. Earth Planet Sci Lett 302:227–235
47. Yavorski BM, Detlaf AA (1977) Handbook of physics. Mir, Moscow, pp 866–867
48. Ikeya M (2002) New applications of electron spin resonance—dating dosimetry and microscopy. World Scientific, Singapore
49. Aitken MJ (1990) Science-based dating in archaeology. Longman, New York
50. Friedman I, Smith RL (1960) A new dating method using Obsidian: part I, the development of the method. Am Antiquity 25:476–522
51. Belyustin AA (2011) The centenary of glass electrode: from Max Cremer to F. G. K. Baucke. J Solid State Electrochem 15:47–65
52. Scholz F (2011) Nikolsky's ion exchange theory versus Baucke's dissociation mechanism of the glass electrode. J Solid State Electrochem 15:67–68
53. Scholz F (2011) From the Leiden jar to the discovery of the glass electrode by Max Cremer. J Solid State Electrochem 15:5–14
54. Stevenson CM, Novak SW (2011) Obsidian hydration dating by infrared spectroscopy: method and calibration. J Archaeol Sci 38:1716–1726
55. Anovitz LM, Elam M, Riciputi L, Cole D (1999) The failure of obsidian hydration dating: sources, implications, and new directions. J Archaeol Sci 26:735–752
56. Friedman I, Trembour FW (1983) Obsidian hydration dating update. Am Antiquity 48:544–547
57. Freter AC (1993) Obsidian-hydration dating: its past, present, and future application in Mesoamerica. Anc Mesoam 4:285–303
58. Liritzis I, Diakostamatiou M (2002) Towards a new method of obsidian hydration dating with secondary ion mass spectrometry via a surface saturation layer approach. Archaeometry 2:3–20
59. Riciputi LR, Elam JM, Anovitz LM, Cole DR (2002) Obsidian diffusion dating by secondary ion mass spectrometry: a test using results from Mound-65, Chalco, Mexico. J Archaeol Sci 29:1055–1075
60. Stevenson C, Liritzis I, Diakostamatiou M (2002) Investigations towards the hydration dating of Aegean obsidian. Mediterr Archaeol Archaeom 2:93–109
61. Liritzis I, Bonini M, Laskaris N (2008) Obsidian hydration dating by SIMS-SS: surface suitability criteria from atomic force microscopy. Surf Interf Anal 40:458–463
62. Liritzis I, Laskaris N (2011) Fifty years of obsidian hydration dating in archaeology. J Non-Cryst Solids 357:2011–2023
63. Bada JL, Luyendyk BP, Maynard JB (1970) Marine Sediments: dating by the racemization of amino acids. Science 170:730–732
64. Hare PE, Mitterer RM (1967) Nonprotein amino acids in fossil shells. Yearb Carnegie Inst Wash 65:362–364
65. Hare PE, Abelson PH (1968) Abelson, racemization of amino acids in fossil shells. Yearb Carnegie Inst Wash 66:526–528
66. Hare PE, Mitterer RM (1969) Laboratory simulation of amino-acid diagenesis in fossils. Yearb Carnegie Inst Wash 67:205–208
67. Bada JL (1985) Amino acid racemization dating of fossil bones. Ann Rev Earth Planetary Sci 13:241–268
68. Poinar HN, Hoss M, Bada JL, Paabo S (1996) Amino acid racemization and the preservation of ancient DNA. Science 272:864–866
69. Johnson BJ, Miller GI (1997) Archaeological applications of amino acid racemization. Archaeometry 39:265–287
70. Canoira L, Garcia-Martinez M-J, Llamas JF, Ortiz JE, De Torres T (2003) Kinetics of amino acid racemization (epimerization) in the dentine of fossil and modern bear teeth. Int J Chem Kinetics 35:576–591

71. Ogino T, Ogino H (1988) Application to forensic odontology of aspartic acid racemisation in unerupted and supernumerary teeth. J Dent Sci 67:1319–1322
72. Reich S, Leitus G, Shalev S (2003) Measurement of corrosion content of archaeological lead artifacts by their Meissner response in the superconducting state; a new dating method. New J Phys 5:99.1–99.9
73. Doménech-Carbó A, Doménech-Carbó MT, Peiró-Ronda MA (2011) Dating archaeological lead artifacts from measurement of the corrosion content using the voltammetry of microparticles. Anal Chem 83:5639–5644
74. Doménech-Carbó A, Doménech-Carbó MT, Peiró-Ronda MA, Martínez-Lázaro I, Barrio J (2012) Application of the voltammetry of microparticles for dating archaeological lead using polarization curves and electrochemical impedance spectroscopy. J Solid State Electrochem 16:2349–2356
75. Doménech-Carbó A, Doménech-Carbó MT, Capelo S, Pasíes T, Martínez-Lázaro I (2014) Dating archaeological copper/bronze artifacts using the voltammetry of microparticles. Angew Chem Int Ed 53:9262–9266
76. Scholz F, Schröder U, Gulaboski R, Doménech-Carbó A (2014) Electrochemistry of immobilized particles and droplets, 2nd edn. Springer, Berlin, Heidelberg
77. Doménech-Carbó A, Labuda J, Scholz F (2013) Electroanalytical chemistry for the analysis of solids: characterization and classification (technical report). Pure Appl Chem 85:609–631
78. Doménech-Carbó A, Doménech-Carbó MT, Costa V (2009) Electrochemical methods applied to archaeometry, conservation and restoration. In: Scholz F (ed) Monographs in electrochemistry series. Springer, Berlin, Heidelberg
79. Scholz F, Schröder U, Meyer S, Brainina KhZ, Zakharchuk NF, Sobolev NV, Kozmenko OA (1995) The electrochemical response of radiation defects of non-conducting materials An electrochemical access to age determinations. J Electroanal Chem 385:139–142
80. Doménech-Carbó A, Doménech-Carbó MT, Lee Y, Osete-Cortina L (2012) Potential application of voltammetry of microparticles for dating porcine blood-based binding media used in Taiwanese architectural polychromies. Chem Asian J 7:2268–2273
81. Zuckerkandl E, Pauling LB (1962) Molecular disease, evolution, and genic heterogeneity. In: Kasha M, Pullman B (eds) Horizons in Biochemistry. Academic Press, New York, pp 189–225
82. Margoliash E (1963) Prmary structure and evolution of cytochrome C. Proc Natl Acad Sci USA 50:672–679
83. Kimura M (1968) Evolutionary rate at the molecular level. Nature 217:624–626
84. Ayala FJ (1999) Molecular clock mirages. Biassays 21:71–75
85. Ho SYW, Phillips MJ, Cooper A, Drummond AJ (2005) Time dependency of molecular rate estimates and systematic overestimation of recent divergence times. Mol Biol Evol 22:1561–1568
86. Schwartz JH, Maresca B (2006) Do molecular clocks run at all? A critique of molecular systematics. Biol Theor 1:357–371
87. Drummond AJ, Ho SYW, Phillips MJ, Rambaut A (2006) Relaxed phylogenetics and dating with confidence. PLoS Biol 4:e88
88. Horvath S (2013) DNA methylation age of human tissues and cell types. Genome Biol 14:R115